AD NUMBER
AD479615
LIMITATION CHANGES
TO: **Approved for public release; distribution is unlimited.**
FROM: **Distribution authorized to U.S. Gov't. agencies and their contractors; Administrative/Operational Use; MAR 1966. Other requests shall be referred to Rocket Propulsion Lab., Edwards AFB, CA.**
AUTHORITY
AFRPL ltr 10 Dec 1985

AD 479 615

AUTHORITY:
AFRPL ltr. 10 Dec 85

Tech. Report No. AFRPL-TR-66956

FLAME TEMPERATURE MEASUREMENT OF METALIZED PROPELLANT

Prepared by

S. E. Colucci and
J. M. Adams
Aerojet-General Corporation

March 1966

Prepared for

ROCKET PROPULSION LABORATORY
Air Force Systems Command
Edwards, California

"When U. S. Government drawings, specifications or other data are used for any purpose other than a definitely related Government procurement operation, the government thereby incurs no responsibility or any obligation whatsoever, and the fact that the government may have formulated, furnished, or in any way supplied the said drawing, specification, or other data, to be regarded by implication or otherwise, or in any matter likewise the holder or any other person or corporation, or convey any right or permission to manufacture, use, or sell any patented invention that may in any way be related thereto."

This document is subject to special export controls and each transmittal to foreign governments or foreign nationals may be made only with prior approval of AFRPL (RPPR-STIN-FO), Edwards, California, 93423.

The report number shown on this document is incorrect.

The correct designation is AFFDL-TR-66-56.

ERRATA

Tech Report AFRPL-TR-66956

There is a consistent error in the equations in this report; a minus sign is missing in the exponential groups of the form

$$\exp\left(\tilde{N}\,\gamma_{ai} + \gamma_g\right) t$$

$$\exp\left(\tilde{N}\,\left(\gamma_{ai} + \gamma_{si}\right) + \gamma_g\right) t\,,$$

$$\exp\left(\tilde{N}\,\left(\gamma_{ai} + \gamma_{si}\right)\,t\right)$$

and $\exp\left(\tilde{N}\,\gamma_{ai}\,t\right),\ i = 1,2,$

which appear on pp. 8,9 and on p.2 of the Appendix. The groups should include a minus sign, thusly:

$$\exp\left[-\left(\tilde{N}\left(\gamma_{ai} + \gamma_{si}\right) + \gamma_g\right) t\right],$$

$$\exp\left[-\left(\tilde{N}\,\gamma_{ai}\,t\right)\right]\ ,\ \text{etc}$$

Equation 7 of the Appendix should read:

$$\tilde{N}\left(\gamma_{ai} + \gamma_{si}\right)t = -\ln\left[\frac{E_{11}K_{11} - E_{12}K_{12}}{E_{10}K_{10}}\right]$$

March 1966

FLAME TEMPERATURE MEASUREMENT OF METALIZED PROPELLANT

By

S. E. Colucci and J. M. Adams

Prepared for

ROCKET PROPULSION LABORATORY
Air Force Systems Command
Edwards, California

AEROJET-GENERAL CORPORATION
A SUBSIDIARY OF THE GENERAL TIRE & RUBBER COMPANY

1000T

FOREWORD

This is the third quarterly report of work performed on Contract AF 04(611)-10545, Project No. 3148, BPSN 314803, and program structure No. 750G, covering the period from 19 November 1965 through 18 February 1966. Mr. Curtiss Selph is project engineer at the Rocket Propulsion Laboratory at Edwards, California. Mr. S. E. Colucci is program manager and Dr. J. M. Adams is principal investigator at Aerojet-General Corporation, Sacramento, California.

Publication of this report does not constitute Air Force approval of the report's findings or conclusions. It is published only for the exchange and stimulation of ideas.

ABSTRACT

This third quarterly technical report presents a discussion of the program progress since the previous report of the Flame Temperature Measurement Program. The program includes laboratory development of the temperature measurement technique, test motor development, and results of motor tests and laboratory experiments.

Results of laboratory measurements of spectral absorption cross sections are presented and are used to calculate values of the imaginery part of the refractive index for molten alumina. Other results, obtained from the literature are also used as a comparison.

A discussion of the experimental program using small solid rocket motors is presented. The experimental effort includes results of light scattering studies, and gas and particle temperature measurements on the exhaust plume of these small motors.

TABLE OF CONTENTS

APPENDIX

TABLE LIST

FIGURE LIST

FIGURE LIST (cont.)

I.

INTRODUCTION

A. OBJECTIVES

The immediate objective of this program is to develop a method for measuring chamber and exhaust temperatures of metalized propellants and to distinguish between the temperatures of both the gaseous and condensed species in a rocket motor exhaust.

The specific objective is to utilize the measurement techniques developed in this program for those propellants specified in Exhibit A of this contract to gain insight into the actual performance potential of such systems and into methods of improving their performance.

A secondary objective is to obtain thrust and chamber pressure measurements on small motor tests to correlate measured thrust and specific impulse with the measurements of temperature.

B. TECHNICAL APPROACH

The method selected for the measurement of both gas and particle temperature in a rocket motor is the spectral comparison method. This method utilizes spectrometric measurements of radiation intensity from the flame and particles to determine the electronic temperature of the gas and the surface temperature of the particles.

The necessary equipment for the assembly of the spectral comparison pyrometer (SCP) consists of a carbon arc lamp, motorized light choppers, a spectrometer, and a light detection scheme. These components and their function have been described in detail in Reference 1, and further description will not be given in this report.

The period of nine months preceding this report was spent in developing and refining the measurement techniques and equipment by performing a systematic set of spectroscopic and light scattering measurements on an Al_2O_3-particle-laden hydrogen-oxygen flame. Results on random error determination, thermodynamic disequilibrium studies, and light scattering measurements were reported previously (References 1 and 2).

Briefly, the results of the random error determination indicated a confidence interval about temperature typified by the following:

With no particles in the flame:

$$T_g = 2600 \pm 40\ K\ (\nu = 15 \text{ degrees of freedom})$$

With particles in the flame:

$T_g = 2600 \pm 65°K$ (~ 25 degrees of freedom)

$T_p = 2600 \pm 100°K$ (~ 25 degrees of freedom)

The confidence interval about particle temperature does not include the uncertainty in Al_2O_3 refractive index or particle size which causes a larger interval. Further work is continuing on the imaginary part of the refractive index for alumina in the molten state. Data from the laboratory and elsewhere (Reference 3) bear on this problem and will be discussed below. These uncertainties do not affect the gas temperature variance but the present uncertainty in alumina refractive index broadens σ_{T_p} to 200°K.

The results from the experiments on thermodynamic equilibrium in hydrogen-oxygen flames were obtained by studying emission from the spectral lines of barium, cesium, lithium, and sodium. It was found that barium and cesium were poor trace elements to be used for the spectral comparison method of flame temperature measurement, but that sodium and lithium appeared to be satisfactory (Reference 2). Subsequent measurements on small rocket motors have been performed on the first line of the sodium doublet (0.588995μ). The results of the motor tests are described herein.

Light scattering measurements on a particle-laden flame were related to effective particle size and number concentration through Mie scattering theory. Particle size distribution determined from microscopic examination of a sample collected from the flame was in striking agreement with that determined from the optical measurements. A further check on number concentration was possible because the mass flow rate of particles was monitored. Again, the agreement with that value of number concentration obtained from the optical measurements was very good and a good confidence in the light scattering measurement technique was established.

Motor firings were then conducted with measurements of spectral emission and scattered light intensity being recorded in the exhaust plume just past the exit plane of the motor. Initially, ancillary equipment was fabricated and installed to allow three sequential spectroscopic measurements to be taken at different axial locations during the firing (Reference 1). It was learned from the first two motor firings that the reference light source when coupled to the ancillary equipment was of insufficient intensity to allow determination of the plume extinction coefficient. Upon eliminating a portion of the ancillary equipment, successful measurements at one axial station were made which are discussed in the following paragraphs. Hence, the remainder of the motor tests of this program will be conducted with temperatures measured at either the chamber or in the nozzle exhaust plume.

II.

TECHNICAL DISCUSSION

A. ANALYSIS

The analyses of the spectroscopic and optical scattering measurements to determine gas and particle temperature has been continued during the last three-month period. Previous quarterly reports, References 1 and 2, have included the following analytical studies:

1. Principles of SCP operation
2. Reduction of spectroscopic data
3. Mie scattering theory
4. Reduction of light scattering data

During the past three-month period, special emphasis has been placed on the difficult problem of determining the refractive index for alumina and the effect of optical depth on the temperatures measured. These analyses are discussed below.

1. Refractive Index of Alumina

As shown in the previous quarterly reports (References 1 and 2), the radiation scattered from particles in two-phase flow must be accounted for in the determination of gas and particle temperature. To do this, Mie scattering theory is used to relate light scattering or extinction measurements to the scattering cross section (v. Appendix C, Reference 1). With a knowledge of particle size distribution, number density of particles and refractive index, it is possible to compute the effective absorption cross section for the particles and the emissivity of the particle cloud.

The refractive index is a complex number, i.e.

$$m = n - n'i$$

where n is a measure of the change in the speed of light in the medium (in this case, $Al_2O_{3(l)}$) relative to the value in the surrounding medium, and n' is related to the absorption or attenuation of the light beam in the medium. Absorption in the medium can be described through the relation

$$I = I_o e^{-\gamma t}$$

where γ is the usual absorption coefficient and t is the thickness. It can be readily shown that n' is related to the absorption coefficient in the medium by the following:

$$\gamma = 2n'k = \frac{4\pi n'}{\lambda} \qquad \text{(Eq 1)}$$

For a system of scatterers it can be shown (although not so readily) that the absorption cross section, γ_a, used to determine the emissivity of the particle cloud by

$$\varepsilon_p = 1 - e^{-\tilde{N}\gamma_a t}, \qquad \text{(Eq 2)}$$

is approximately directly proportional to n', i.e.

$$\gamma_a \propto n' \qquad \text{(Eq 3)}$$

From the above it is obvious that in order to obtain accuracy in the determination of particle temperature, n' must be known to within close limits. Table 1 indicates the dependence of T_p on n', using the data from motor firing Nc. 3.

TABLE 1

DEPENDENCE OF T_p ON n'

n = 1.7999 (Reference 4)

T_p(0.1 sec),* °K	T_p(0.7 sec),* °K	n'
3662	3805	0.0005
3332	3453	0.001
2804	2899	0.005

*Time refers to elapsed time from start of firing.

If these were the only measurements of temperature available to us, we would suspect that n' >0.001, since for values of n' less than 0.001, the temperatures determined from the spectral measurements appear to be excessively high. Data obtained by Gryvnak and Burch (Reference 5) indicate that a value of $\gamma = 1$ mm^{-1} is likely at the melting temperature, where they observed a sharp increase in the alumina emmittance. Unfortunately, they could not measure the thickness of the molten sample and hence could not determine γ to a reasonable precision. However, using the value of $\gamma = 1$ mm^{-1}:

$$n' = \frac{\lambda\gamma}{4\pi} = 0.00008 \text{ at } 1\mu$$

Fortunately there are other measurements on Al_2O_3 particle cloud emittance which can be used. These were obtained in the early portion of this program, where Al_2O_3 particles were injected into a H_2/O_2 flame at temperature from 2600°K to 3000°K. These measurements of emittance were reduced using the particle distribution determined by sampling and light scattering measurements (Reference 2). They are presented in Table 2; data from Reference 6 is presented in Table 4.

TABLE 2

n' FOR MOLTEN ALUMINA, OBTAINED FROM EXPERIMENTS ON FLAMES CONTAINING PARTICLES

Calculated γ_a, Mie Scattering Theory[2]:

γ_a ($\lambda = 0.588\mu$)	n'
1.1508×10^{-13} cm^2	0.0001
5.7435×10^{-13}	0.0005
1.146×10^{-12}	0.001
5.623×10^{-12}	0.005
1.099×10^{-11}	0.01

Measured γ_a, Experiments on H_2/O_2 flames[3]:

Run	γ_a ($\lambda = 0.588\mu$)	T_g (°K)[1]	n'
1	7.2×10^{-12}	2685	0.0079
2	6.1×10^{-12}	2466	0.0043
3	6.5×10^{-12}	2750	0.0072
4	8.5×10^{-12}	2885	0.0094
5	7.6×10^{-12}	2700	0.0084

avg. n' = 0.0074 $\pm$ 0.00055 (2500 - 2900°K)

1 Measured during run with Spectral Comparison Pyrometer
2 Conditions on particle size distribution shown in Table 3
3 Standard deviation on measured $\gamma_a = 0.5 \times 10^{-12}$ for 25-30 degrees of freedom. Calculations are shown in the Appendix.

TABLE 3

PARTICLE SIZE DISTRIBUTION USED IN DETERMINING γ_a OF TABLE 2

$D_{(micron)}$	$f_{(D)(unnormalized)}$
0.0950	0.5440
0.1900	0.1270
0.2850	0.0288
0.3800	0.200
0.4750	0.0144

Number density of particles used in Table 2 computed from

$$\tilde{N} = \frac{\chi \rho_g}{\rho_g \chi + \rho_L (1-\chi)\bar{V}}$$

with $\bar{V} = 2.901 \times 10^{-15}$ cm^3/particle

ρ_g determined from CHEM COMP computer routine at mixture ratio used in run (Reference 7).

χ determined from weight balance on particle before and after run, measured flow rates of gas

ρL determined from Reference 8.

TABLE 4

n' FOR MOLTEN ALUMINA, OBTAINED FROM MEASUREMENTS DESCRIBED IN REFERENCE 6

Calculated γ_a, Mie Scattering Theory[1]:

γ_a		n'
$\lambda = 1.3\mu$	$\lambda = 1.7\mu$	
7.4×10^{-11}	4.17×10^{-11}	0.00005
1.475×10^{-10}	8.336×10^{-11}	0.0001
7.19×10^{-10}	4.15×10^{-10}	0.0005
1.43×10^{-9}	8.32×10^{-10}	0.001
6.95×10^{-9}	4.01×10^{-9}	0.005

Measured γ_a, determined from emittance measurements[2]

$\overline{\gamma}_a$ (all λ)	T(°K)	n' (by interpolation)
1.94×10^{-10}	2320	0.000181
2.74×10^{-10}	2400	0.000258
6.3×10^{-10}	2600	0.000595
1.65×10^{-9}	2800	0.00155
3.33×10^{-9}	3000	0.00326

1 Conditions on particle size distribution from Figure 3 of Reference 6.
2 Calculations are shown in the Appendix. Emittance values obtained by averaging points above 2320°K in Figure 12 of Reference 6.

The results of Reference 6 agree with those of this report to within the uncertainty in all the measurements of both studies. From the data of both Tables 2 and 4, the best value of n' appears to be ∿0.005 for the range of variables used in this study. The recommended refractive index of alumina is given by

$$m = 1.799 - 0.005i \quad (T > \text{melting point of } Al_2O_3,\ \lambda \sim 0.6\mu).$$

2. Effect of Optical Depth on Temperature Measurements

In Reference 1 was presented the theory of the spectral comparison pyrometer in which scattering losses from the control volume were accounted for in the case of emission from the particle cloud. This net loss of radiation would occur only for optically thin regions, or for regions close to a boundary or radiation "sink". For the other extreme, the case of optically thick regions, radiation scattered out of the control volume will be no greater than that scattered back into the volume. This would most probably be the case for an exhaust plume of a small motor like those under study in this program; hence, scattering losses along the optical path subtended by the detection optics need not be considered in the treatment of plume radiation alone. However, with the reference light source on, a net scattering loss of the radiation from a control volume would be expected, because of the anisotropy of the source beam (Reference 9). It will, for the present, be assumed that all the radiation from the reference source beam which is scattered out of a control volume is permanently lost. Actually, because of multiple scattering, some of this radiation is recovered, but that consideration will be reserved for a later treatment.

Equations 4 through 9, relating the gas and particle temperature to the measurements of steradiancy cover the optically thick case just discussed and have been incorporated into the existing computer program (Reference 2) as another option. This option is the one used to reduce the data from the motor firings.

Measured emf, particle emission alone, (at λ_1):

$$E_{12}K_{12} = \tau_{w_1} [1. - \exp(\tilde{N}\gamma_{a1}t)] R_i^o(\lambda_1, T_p) \qquad \text{(Eq 4)*}$$

Measured emf, particle emission plus transmitted reference source beams (at λ_1):

$$E_{11}K_{11} = \tau_{w_1} [1. - \exp(\tilde{N}\gamma_{a1}t)] R_i^o(\lambda_1, T_p) \qquad \text{(Eq. 5)}$$

$$+ \tau_{w_1}^2 [\exp(\tilde{N}(\gamma_{a1} + \gamma_{s1})t)] R_i^o(\lambda_1, T_s)\varepsilon_s(\lambda_1, T_s)$$

* See nomenclature for definition of symbols.

Measured emf, reference source alone:

$$E_{10}K_{10} = \frac{\epsilon_s(\lambda_1,T_s)}{\lambda_1^5\left[\exp\left(\frac{C_2}{\lambda_1 T_s}\right) - 1\right]} \qquad \text{(Eq 6)}$$

Measured emf, particle and gaseous line emission (at λ_2):

$$E_{22}K_{22} = E_{21}K_{21} - \tau_{w_2}^2\left[\exp\left(\tilde{N}\left(\gamma_{a2} + \gamma_{s2}\right) + \gamma_g\right) t\right] \epsilon_s(\lambda_2,T_s)\, R_i^o\,(\lambda_2,T_s) \qquad \text{(Eq 7)}$$

Measured emf, particle, gas emission plus transmitted reference source beam (at λ_2):

$$E_{21}K_{21} = \frac{\tau_{w2}\,\gamma_g}{\tilde{N}\gamma_{a2} + \gamma_g}\left[1 - \exp\left(\tilde{N}\gamma_{a2} + \gamma_g\right) t\right] R_i^o\,(\lambda_2,T_g) + \frac{\tau_{w2}\,\tilde{N}\gamma_{a2}}{\tilde{N}\,\gamma_{a2} + \gamma_g}\left[1 - \exp\left(\tilde{N}\gamma_{a2} + \gamma_g\right) t\right] R_i^o\,(\lambda_2,T_p) + \tau_{w2}^2\left[\exp\left(\tilde{N}\left(\gamma_{a2} + \gamma_{s2}\right) + \gamma_g\right) t\right] R_i^o\,(\lambda_2,T_s)\epsilon_s(\lambda_2,T_s) \qquad \text{(Eq 8)}$$

where

$$R^o\,(\lambda_i,T_j) = \frac{1}{\lambda_i^5\left(\exp\left(\frac{C_2}{\lambda_i T_j}\right) - 1\right)} \qquad \text{(Eq 9)}$$

It has been shown (Reference 9) that the case of extreme optical depth, i.e., where

$$\tilde{N}\gamma_s t >> 1, \qquad \text{(Eq 10)}$$

can best be treated by an effective optical thickness given by

$$t^* = \tilde{N}\gamma_s t^2. \qquad \text{(Eq 11)}$$

This treatment accounts for the greater path length taken by multiple-scattered radiation emitted by the particles and gas in the region under study, and has been incorporated into the existing computer program which is used in reducing the motor firing data.

B. SMALL MOTOR TEST PROGRAM

1. Program Description

To accomplish the stated objectives, nine motor tests were planned. The motor testing program is being conducted in three separate phases distinguished by the type of metalized solid propellant.

Initially, it was planned that the first phase would consist of three 1KS-250 motor tests with an aluminized propellant (ANP 2969) with temperatures measured both in the chamber and at two stations in the exhaust plume. The required ancillary equipment to accomplish the simultaneous measurements was developed, concurrent with the laboratory development of the temperature measurement technique, and utilized in the first two motor tests conducted. From the data of these two tests, it became obvious that the intensity of the carbon arc light source was being attenuated to the point where it could no longer penetrate the propellant gas plume. Hence, the third test was conducted, with RPL concurrence, by eliminating a portion of the ancillary equipment and moving the carbon arc directly to the exhaust gas. The light source penetrated the plume and radiancy measurements were obtained. However, because of a malfunction of an electrical component in the spectrometer, poor precision was realized and a fourth test using the aluminized propellant was conducted before moving into the toxic propellant motor tests. This fourth test was completely successful. Motor thrust, chamber pressure, exhaust gas temperature, exhaust particle temperature, and light scattering measurements were obtained.

In the second phase of this program, these tests of an LM-2 propellant were initially planned before conducting three tests with LMH-2 type propellants in phase III. However, when it became necessary to conduct a fourth aluminized propellant test, the scope of phase II was reduced to two tests and the fourth aluminized motor substituted for the first LM-2 motor test. In addition, it was felt most desirable to obtain early knowledge of the problems to be faced with the LMH-2 type propellants; hence, the fifth test was conducted with this propellant instead of the phase II propellant, LM-2.

In addition to the normal ballistic measurements of chamber pressure and motor thrust, chamber temperature and chamber light scattering were measured through four optical viewports. Exhaust plume light scattering was also measured using a separate light source. These results are discussed in the motor test results section of this report.

2. Description of Equipment

The first two motor tests were conducted with the ancillary equipment and SCP installed, as described in Reference 1, at three axial locations on the motor: one in a plenum in the chamber (downstream from the propellant grain and upstream of the nozzle) and two in the exhaust plume at 0.25 in. and 1.00 in. aft of the exit plane, respectively. Fiber bundles were installed and linked to optical sampling scanners at the reference light source and spectrometer. This allowed successive measurements of steradiancy with and without the reference source radiation passing through the plume. A fourth fiber bundle led directly from the

reference source to the spectrometer to monitor changes in source temperature. This equipment is shown set up in the test cell in Figure 1. A closeup of the motor exhaust with the light scattering measurement equipment is shown in Figure 2. The spectrometer assembly with the sampling switch installed is shown in Figure 3 and a closeup of the carbon arc light source with the optical sampling switch assembly is shown in Figure 4.

Although the optical equipment performed satisfactorily, the results of the first two motor firings indicated that the source beam was being attenuated excessively by the fiber bundles, from refraction at the ends and by absorption. Plume steradiancy was measured, but the determination of particle cloud emissivity was of insufficient precision because of the relatively low transmitted radiancy from the reference source.

For the third motor firing, it was decided to move the carbon arc reference source to a position close to the exhaust plume and make a single measurement at a point approximately 0.5 in. downstream from the exit plane (see Figures 5, 6, and 7). By eliminating the fiber bundles and rotating optics on the carbon arc, the steradiancy from the reference source was increased approximately 15 times.

Postfiring inspection of the motor hardware from the first two tests revealed that the ATJ graphite throat inserts were slightly eroded in the throat vicinity. There was in addition a thin film of deposition (aluminum oxide) on the nozzle exit cone. Pre- and postfiring throat areas are shown in Table 5 for the nozzles tested. The complete aft closure assembly which includes insulators, graphite throat inserts and steel closures were in excellent condition after firing. It was decided to reuse the complete assembly from the second test on the third and then on the fourth motor tests, respectively, with the aluminized propellant. A postfiring view looking aft from the chamber plenum is shown in Figure 8 with optical viewports installed.

It can be seen that the optical viewport assembly tips (adjusting seat) were slightly melted. The components are shown disassembled in Figure 9. The solution was rather straightforward. Flame spraying the AISI 1010 steel adjusting seats with Rokide Z (zirconium oxide) for the third motor firing solved the problem. A postfiring inspection showed that the probe tips came through nicely with no melting. Hence all the probe tips for the remaining motor tests were flame-sprayed with Rokide Z. Soot observed on the transparent windows after firing was attributed to the propellant liner charring due to residual heat in the chamber after the propellant had been consumed.

In order to verify this thesis, window transmissivity measurements were taken on the fourth motor test, which showed that the windows remained clear throughout the firing. A reliable measurement of the time change of window transmissivity, varying from 0.3 to 0.4, was obtained.

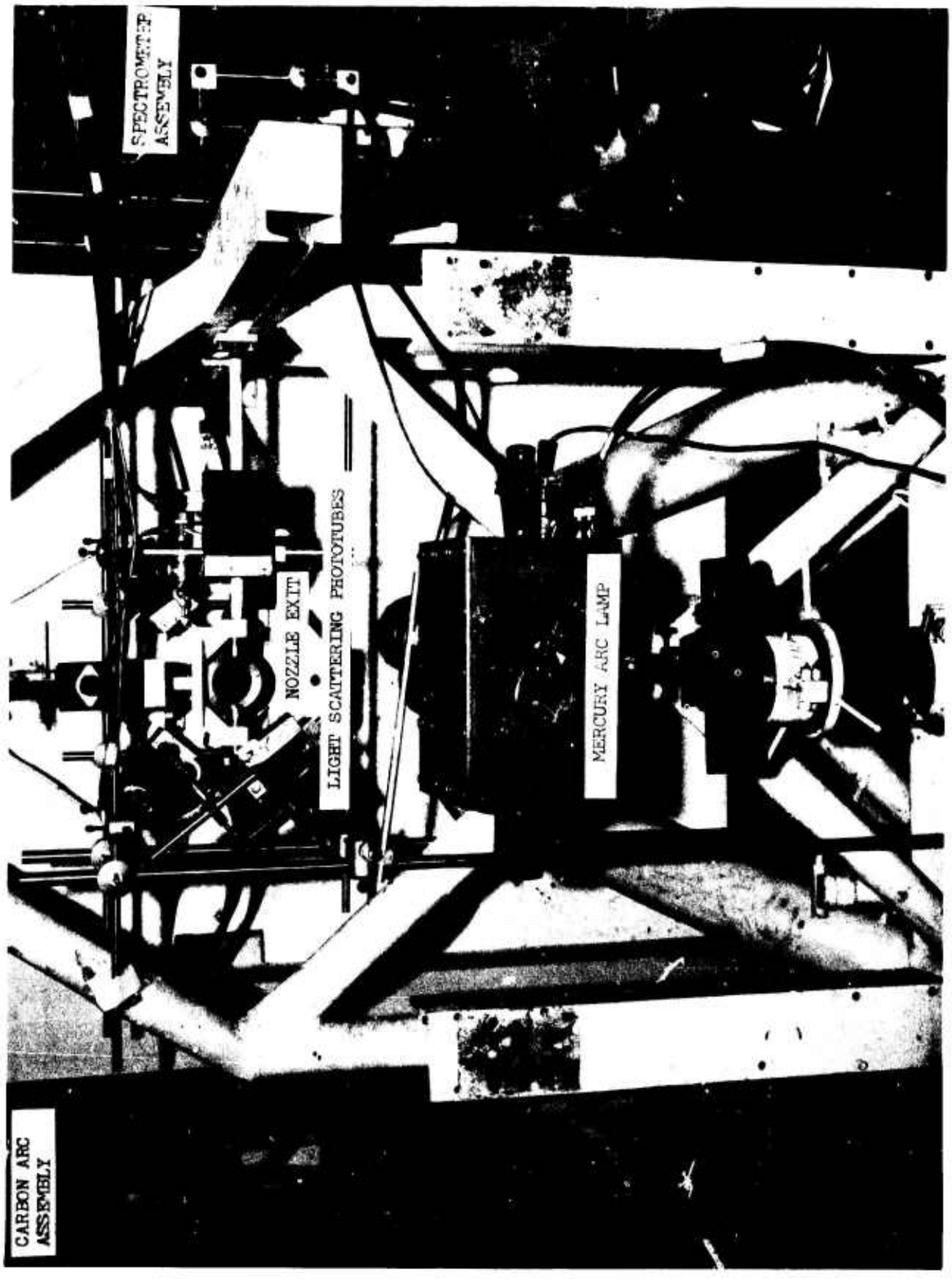

Apparatus Used for Flame Temperature Measurements on Small Motors

Figure 1

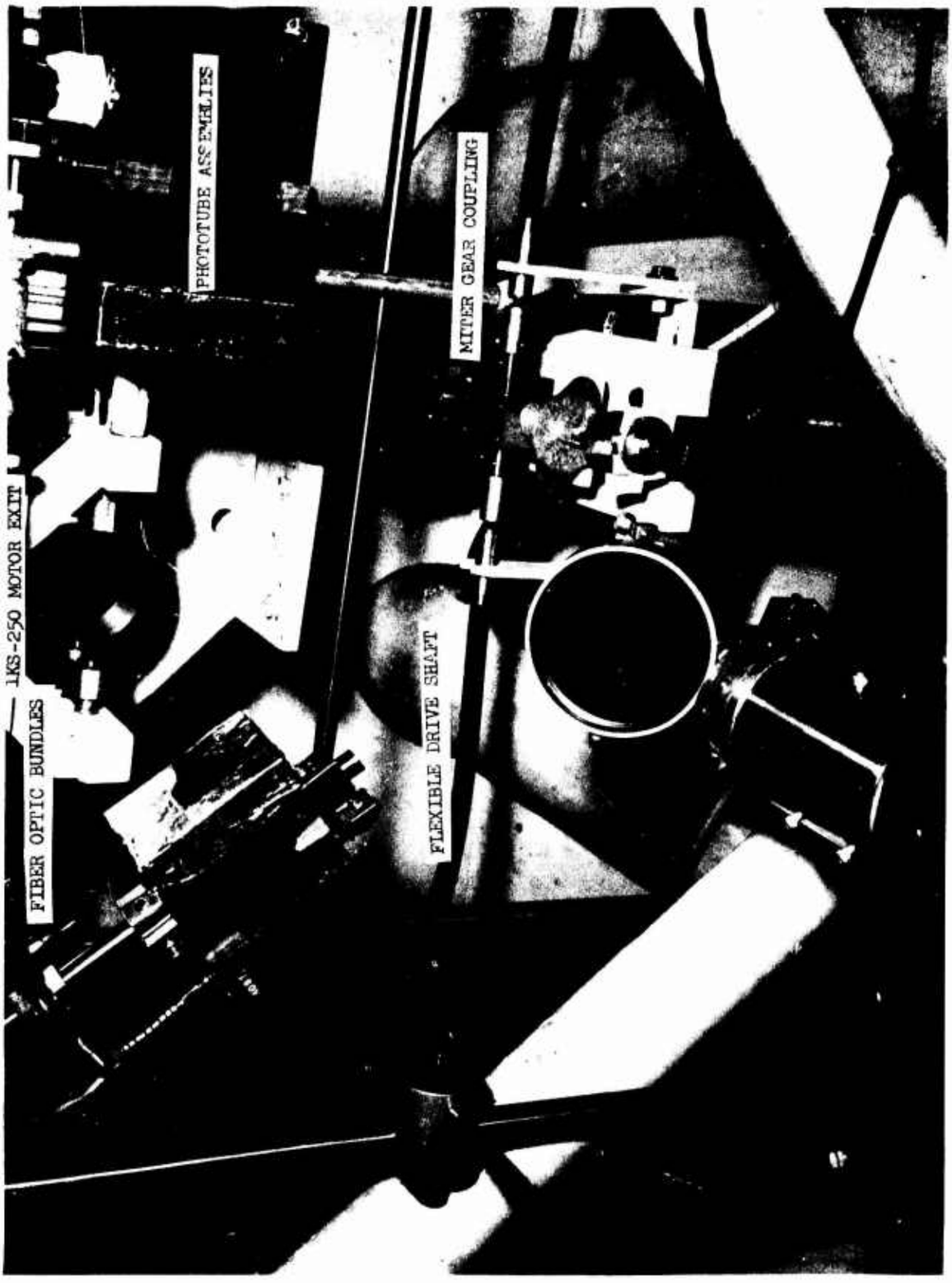

Close-up View of Apparatus

Figure 2

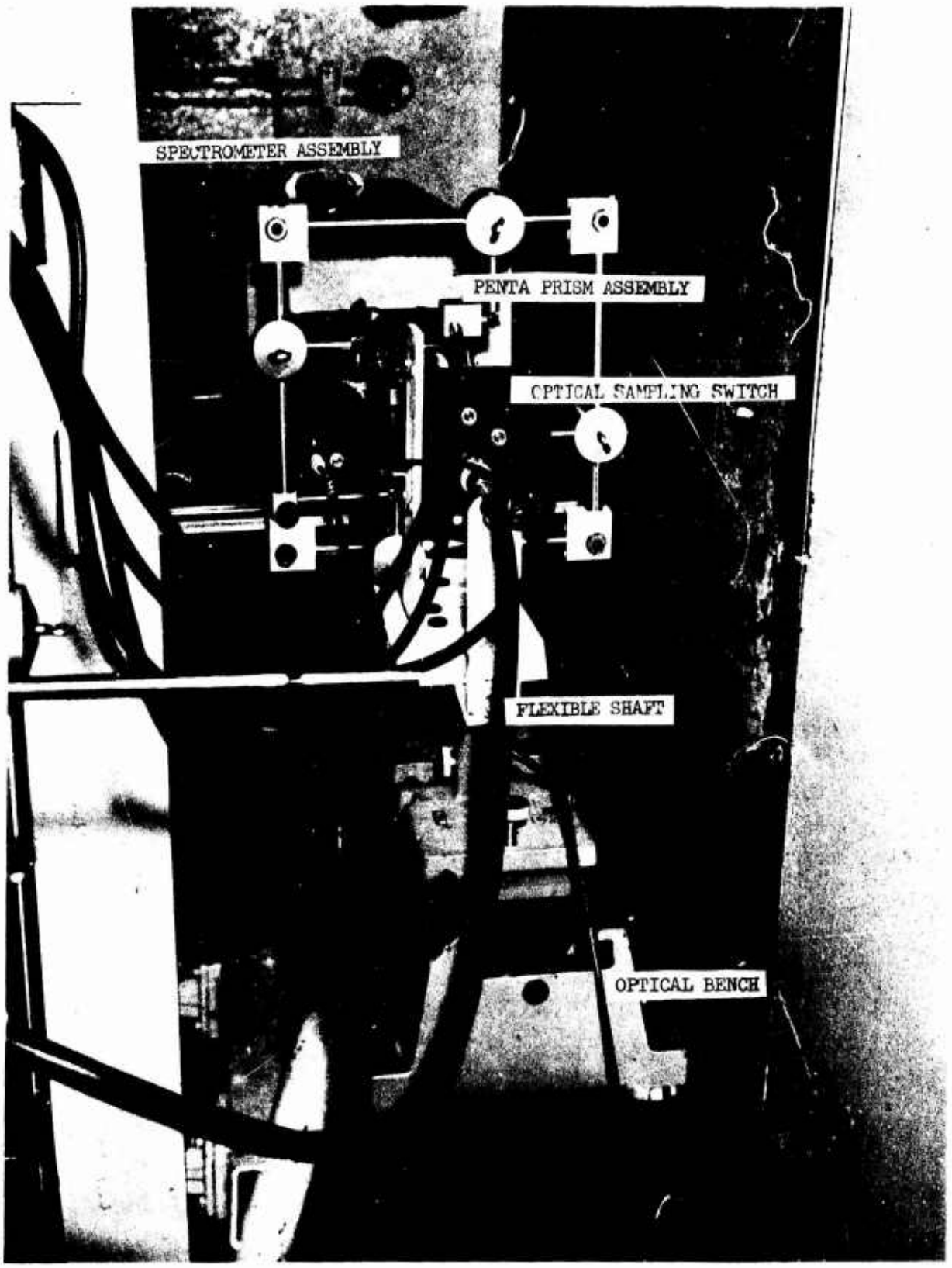

Spectrometer and Optical Sampling Switch Assembly

Figure 3

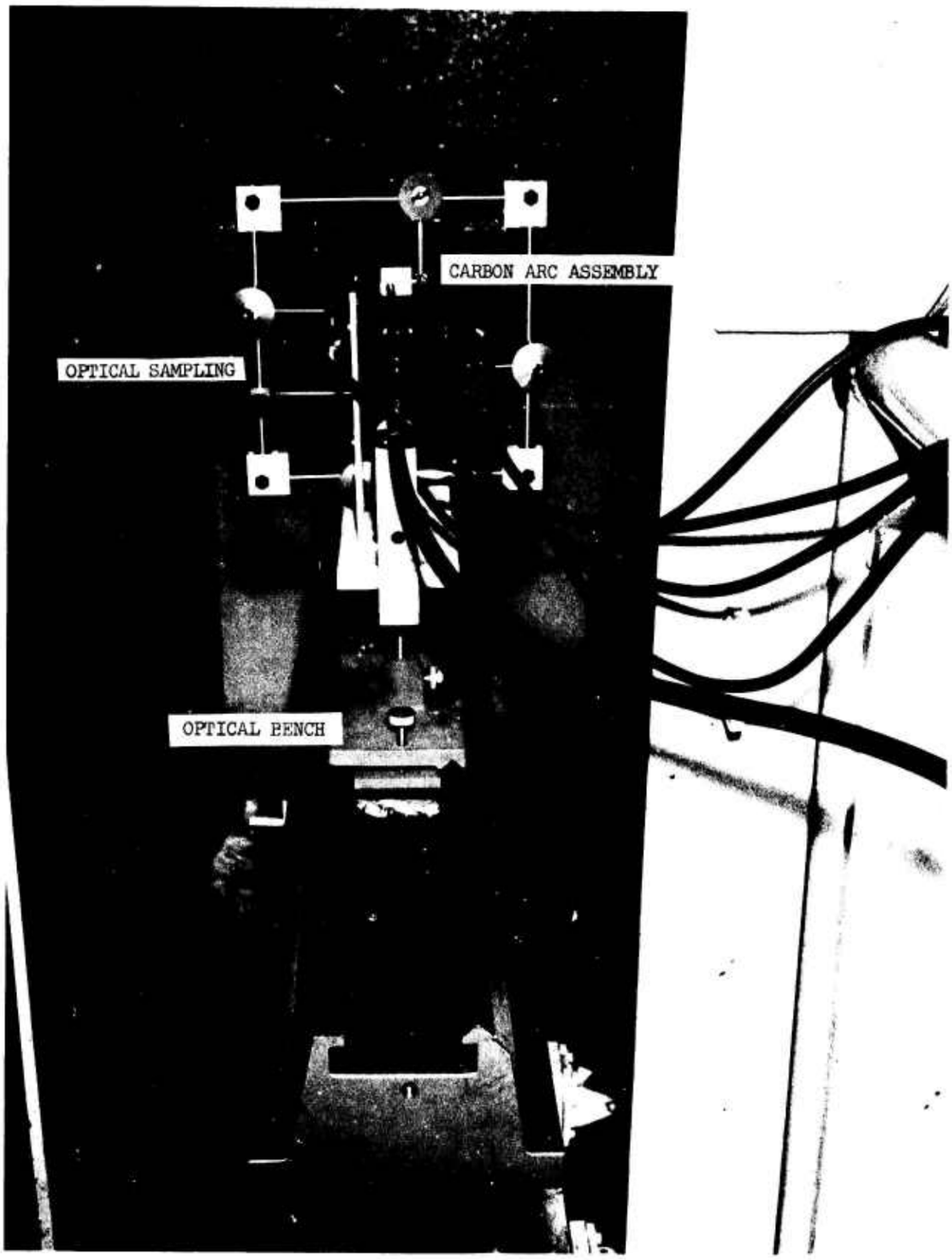

Carbon Arc and Optical Sampling Switch Assembly

Figure 4

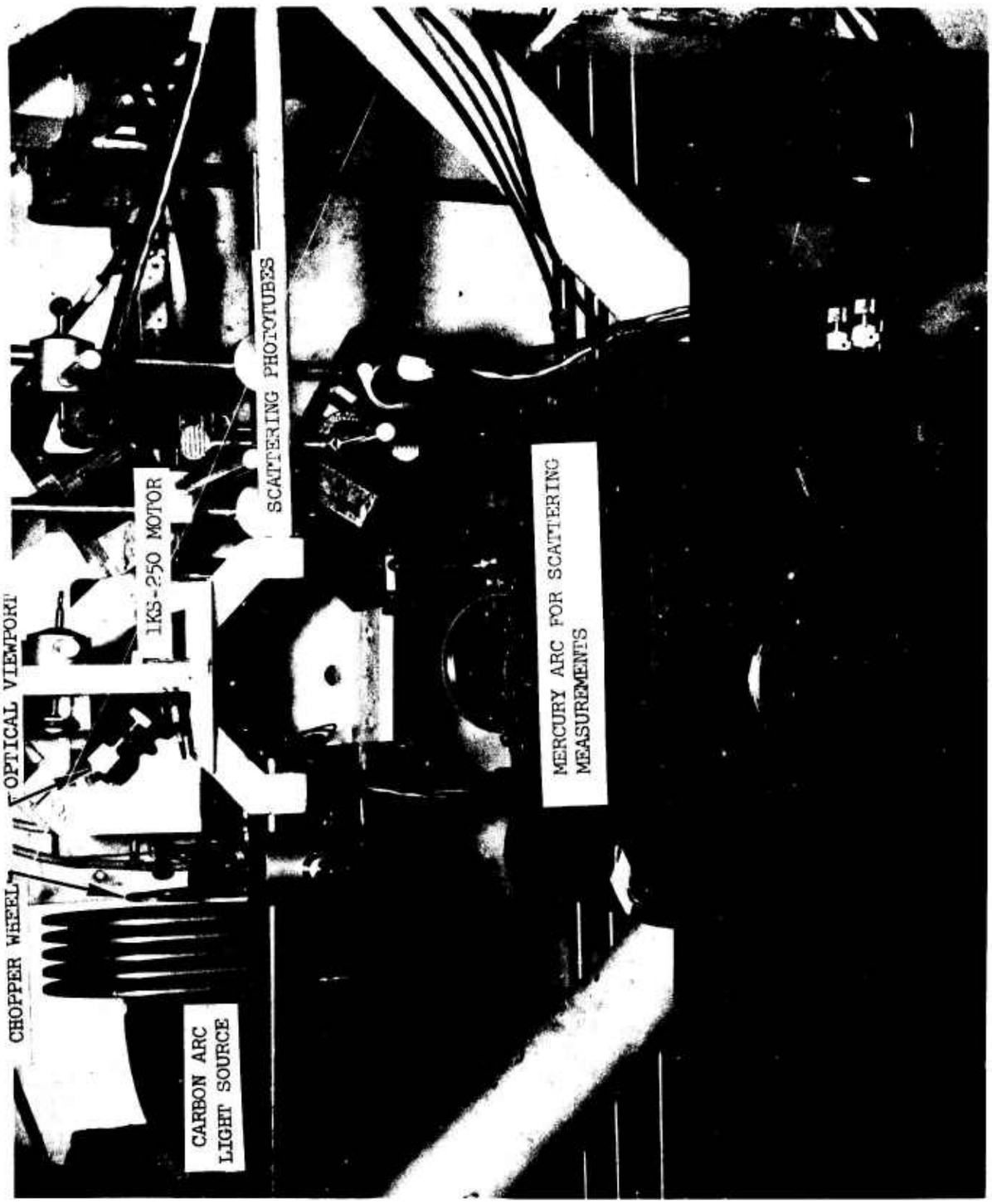

Apparatus Used for Flame Temperature Measurement
on Small Motors

Figure 5

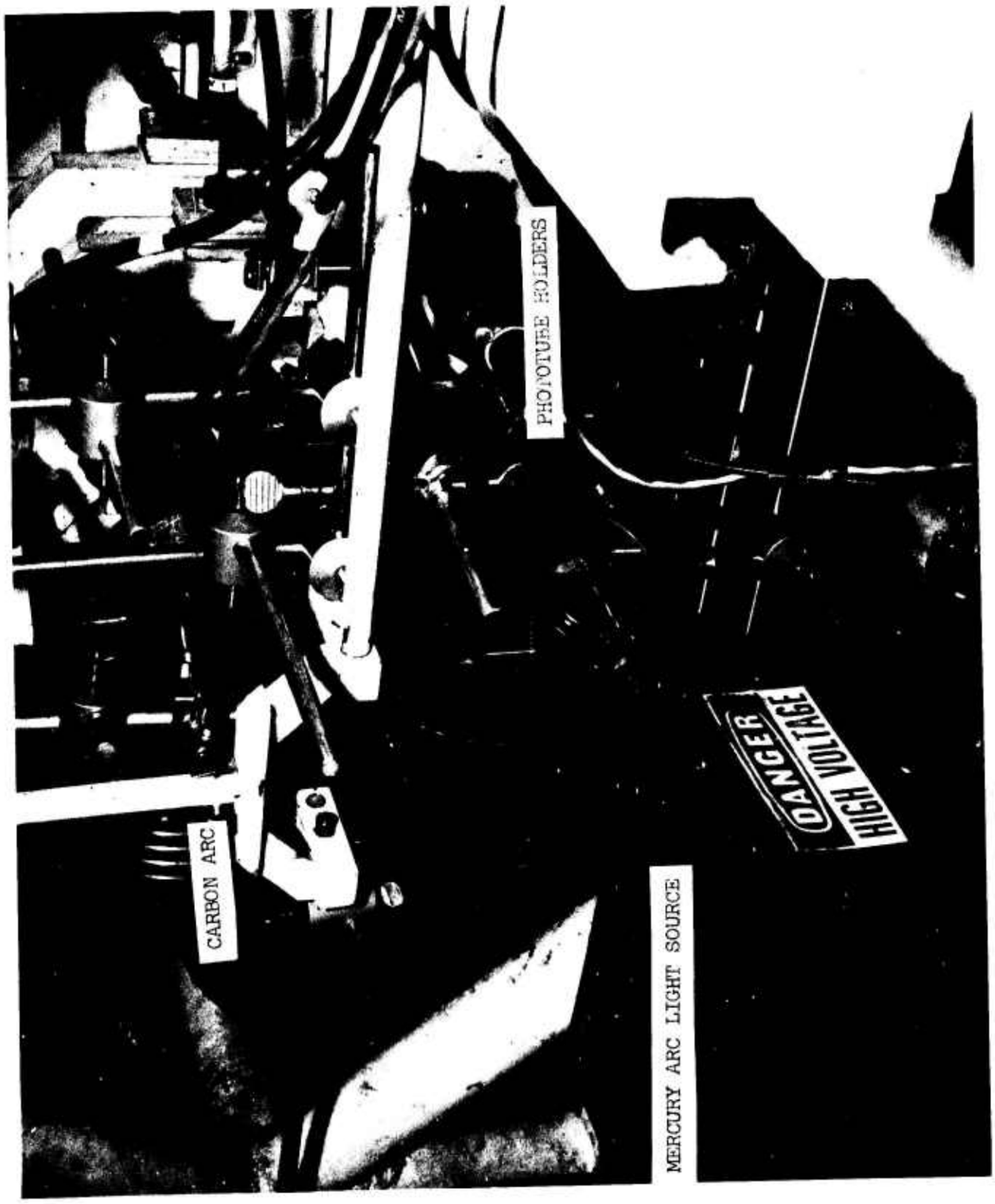

Close-up View of Apparatus

Figure 6

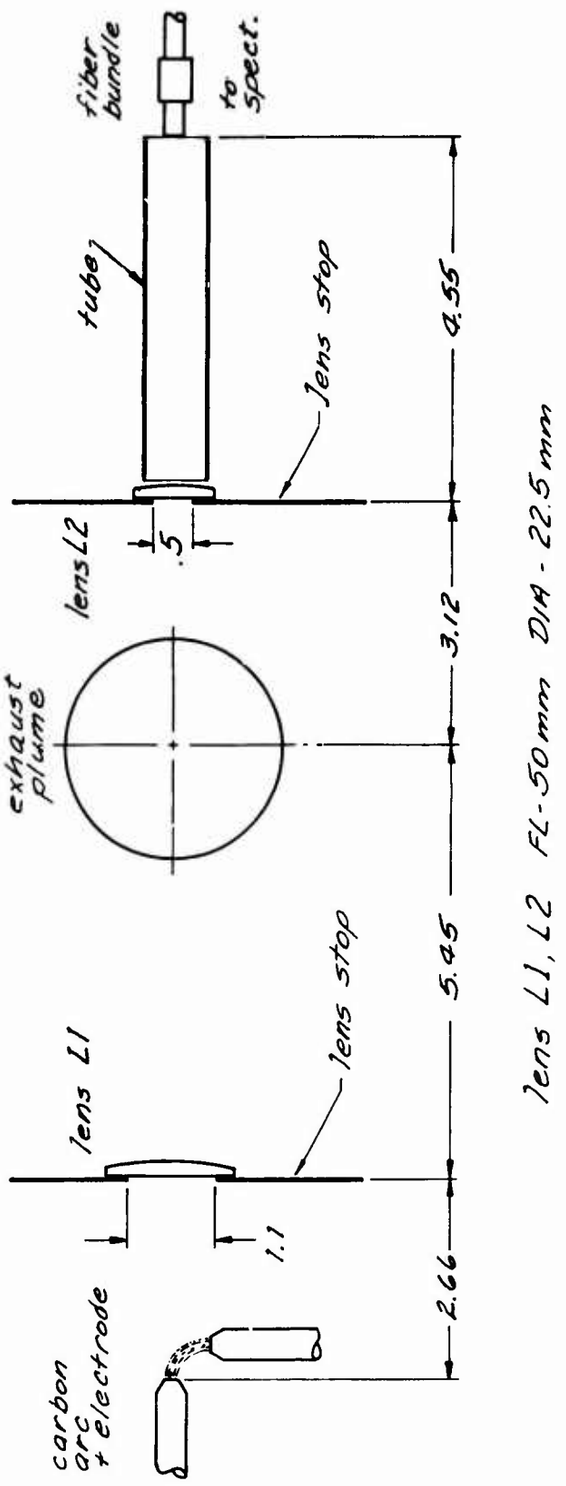

Schematic of Apparatus

Figure 7

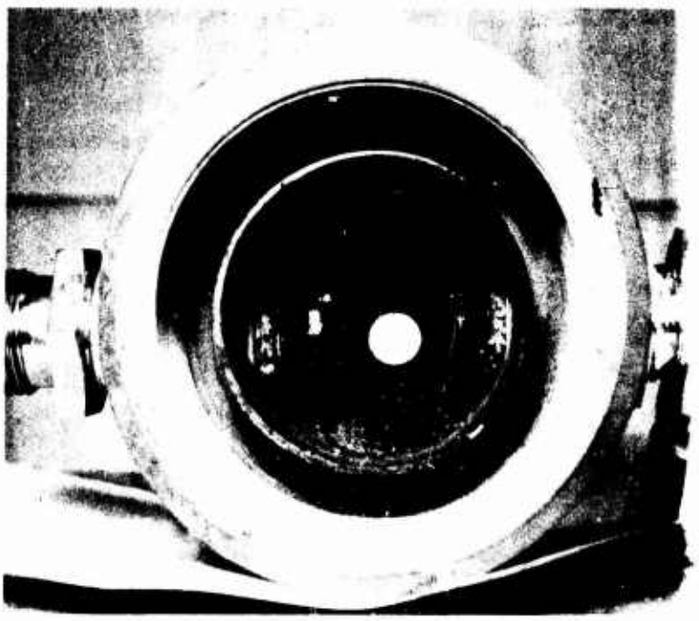

View Looking Aft from Plenum to Throat

Figure 8

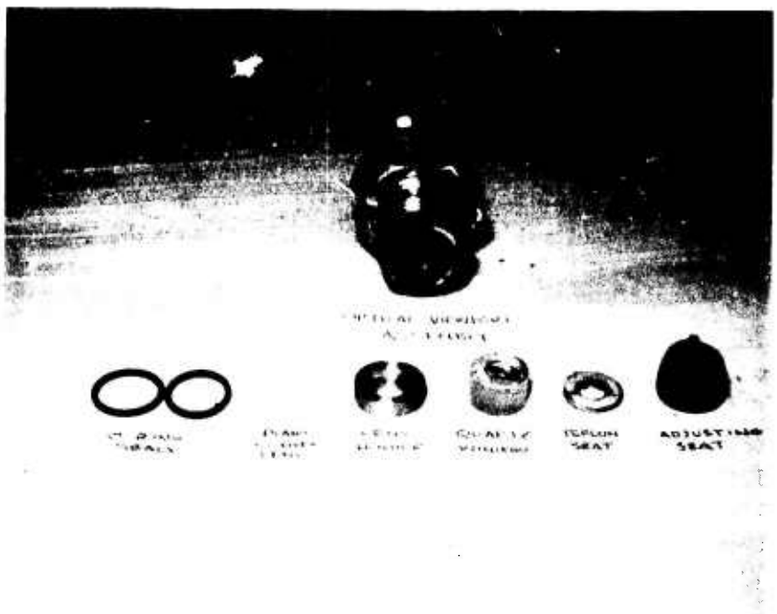

Optical Viewport Components--Postfiring Test No. 2

Figure 9

The transparent window components are shown disassembled after firing in Figure 9. These windows were all pressure- and leak-checked before testing. This was done by immersing one end in water and applying high-pressure nitrogen (800 psia) through a fitting on the other end. Unless the O-rings are seated properly, the window assemblies will not be pressure tight. Leakage was noticed on more than one occasion in the pressure checking. This problem was solved by replacing O-rings and carefully reassembling to ensure proper seating of the O-rings.

3. Motor Test Results

a. Performance Measurements

In addition to the development of techniques for temperature measurement, the secondary objective of this program is to obtain thrust and chamber pressure measurements in order to correlate with the measured temperatures to obtain insight into the actual performance potential of the LMH-2 propellant systems.

These measurements have been obtained on each of the motor firings to date and are shown in Figure 10 through 14. The pressure- and thrust-time curves are integrated to obtain specific impulse and characteristic exhaust velocity. These then, together with the theoretical values, are used to obtain specific impulse efficiency E_{I_s} and characteristic exhaust velocity efficiency E_{C^*}. These will be compared to the thermal efficiency E_t when it is measured with sufficient precision. The motor performance data are summarized in Table 5.

The specific impulse measured at motor conditions is corrected to a standard condition (optimum expansion for 15° conical nozzle from 1000 psia to 14.7 psia) for the aluminized propellant only. This then is divided by the theoretical specific impulse using the shifting equilibrium with solidification option of Reference 7. This does not require a special computer run for each separate test conditon.

Data reduction for the LMH-2 propellants, however, requires a calculation of the theoretical specific impulses at exact motor conditions (average chamber pressure, ambient pressure, and nozzle expansion ratio) and at standard conditions (optimum expansion from 1000-psia chamber pressure to sea-level ambient pressure, and nozzle expansion ratio).

Briefly, the Aerojet computer program (Reference 7) involves an iterative solution of simultaneous equilibrium constants with adiabatic (isenthalpic) combustion at fixed chamber pressure, followed by isentropic flow through the nozzle. The theoretical specific impulse is then calculated from the difference in enthalpy occurring between the chamber and the nozzle exit plane.

The necessary input data required by the computer program includes the heats of formation of the propellant ingredients plus the heats of formation, entropies and heat capacities as a function of temperature for all conceivable combustion products. The latest JANAF data (Reference 12) are used where available and all thermodynamic data for propellant ingredients and combustion products are periodically revised as new data become available.

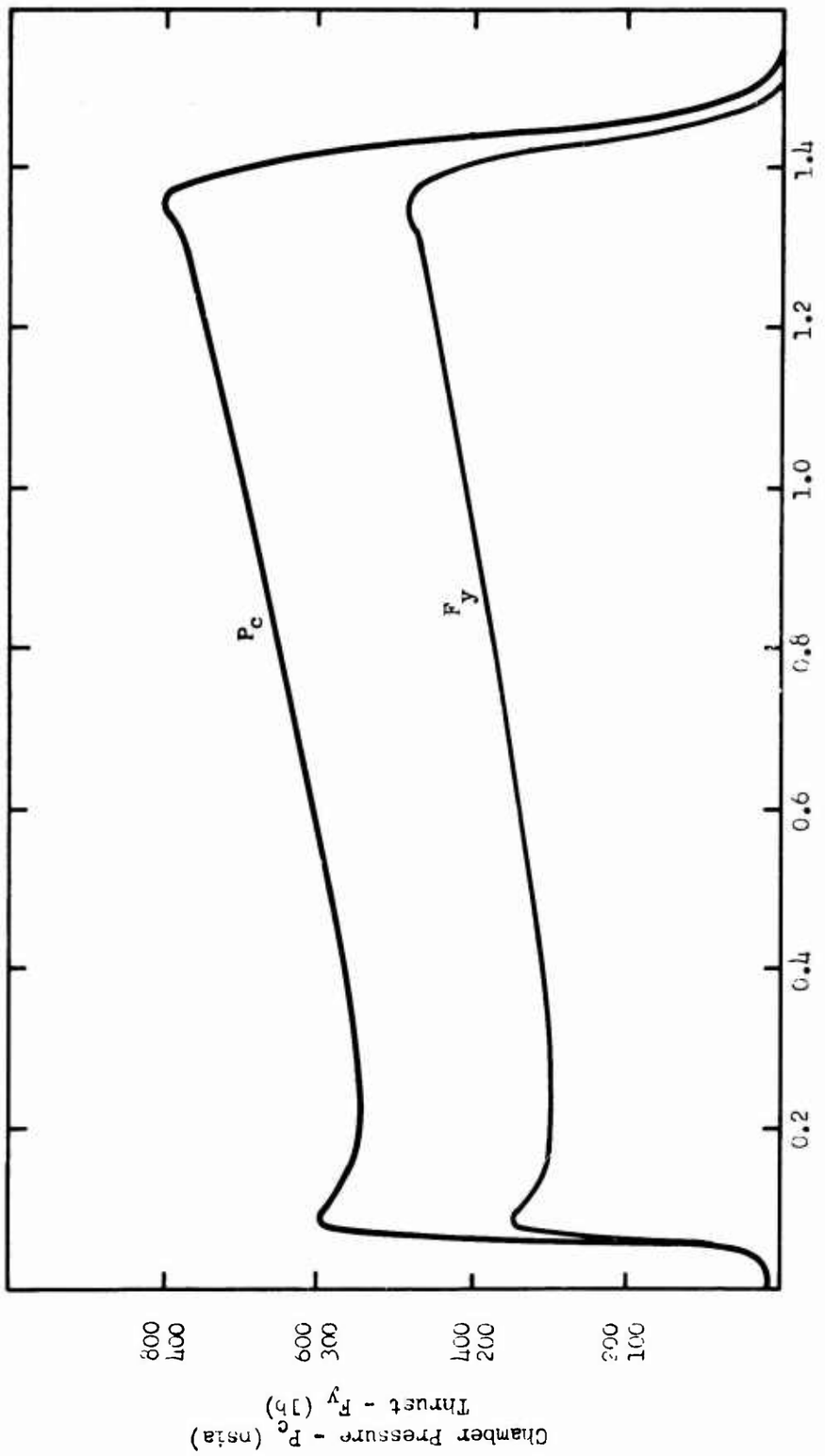

Motor Performance (Test Series FT-ZX-01S-BH-1)

Figure 10

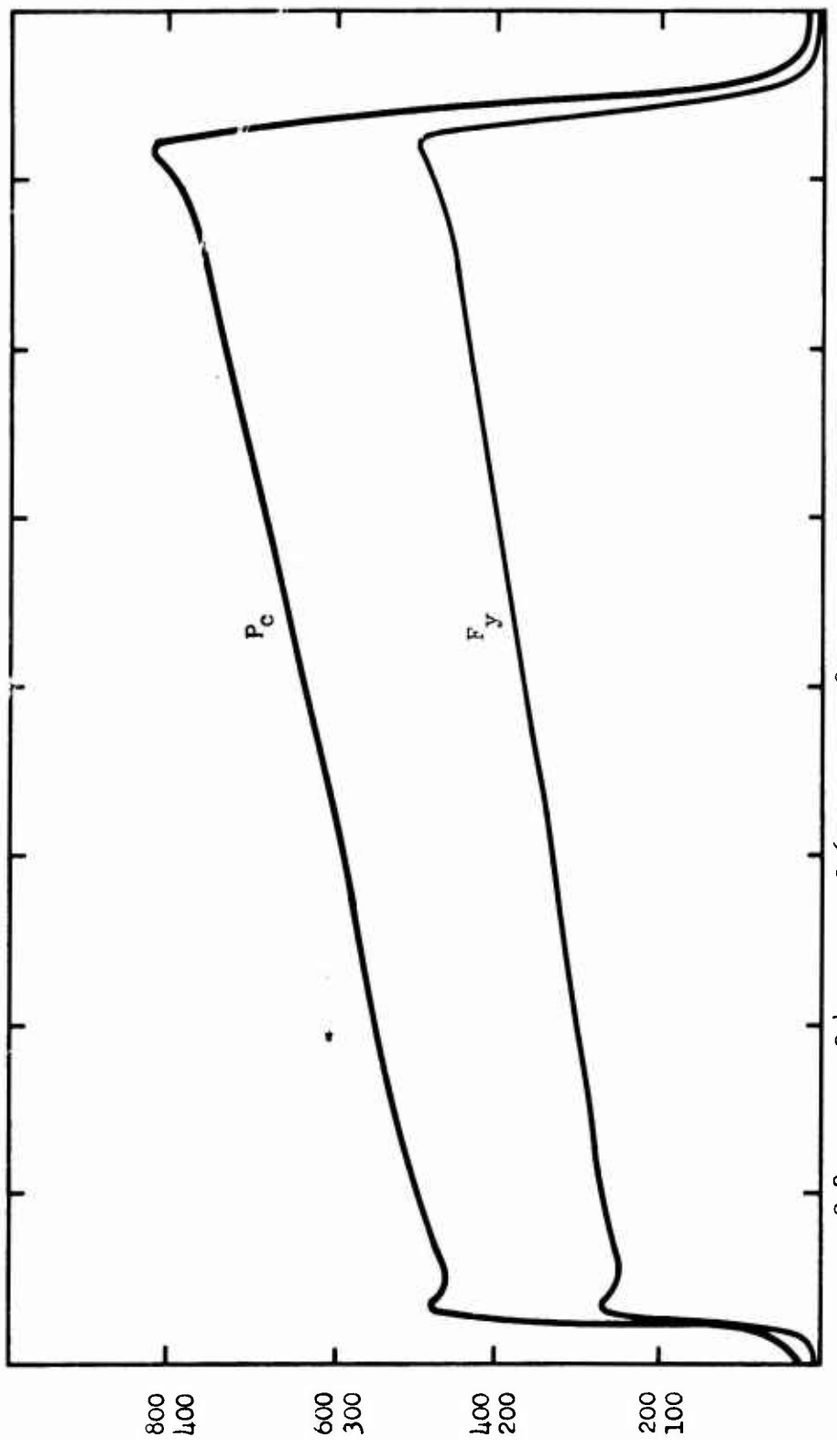

Motor Performance (Test Series FT-ZX-01S-BH-2)

Figure 11

Motor Performance (Test Series FT-ZX-01S-BH-3)

Figure 12

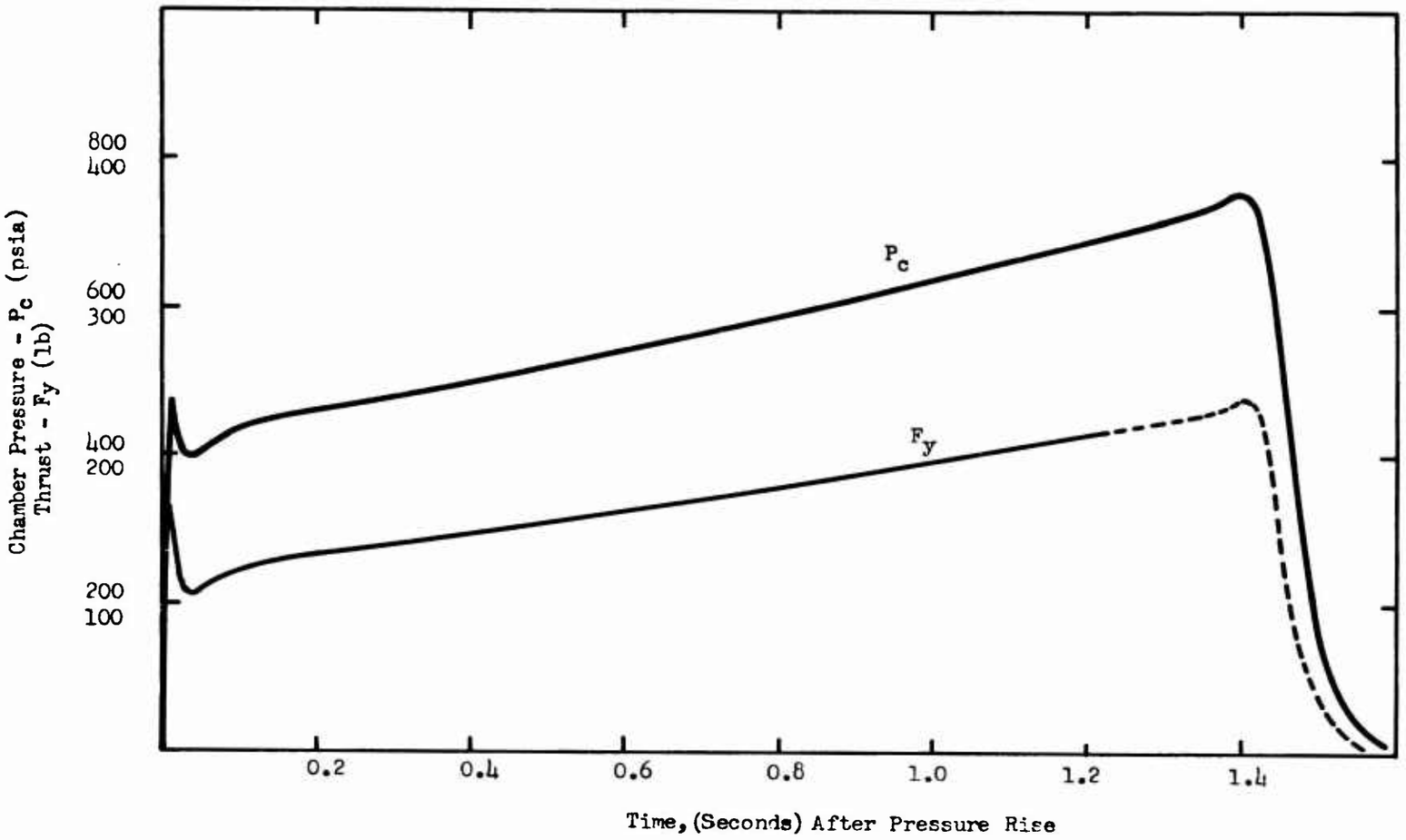

Motor Performance (Test Series FT-ZX-01S-BH-5)

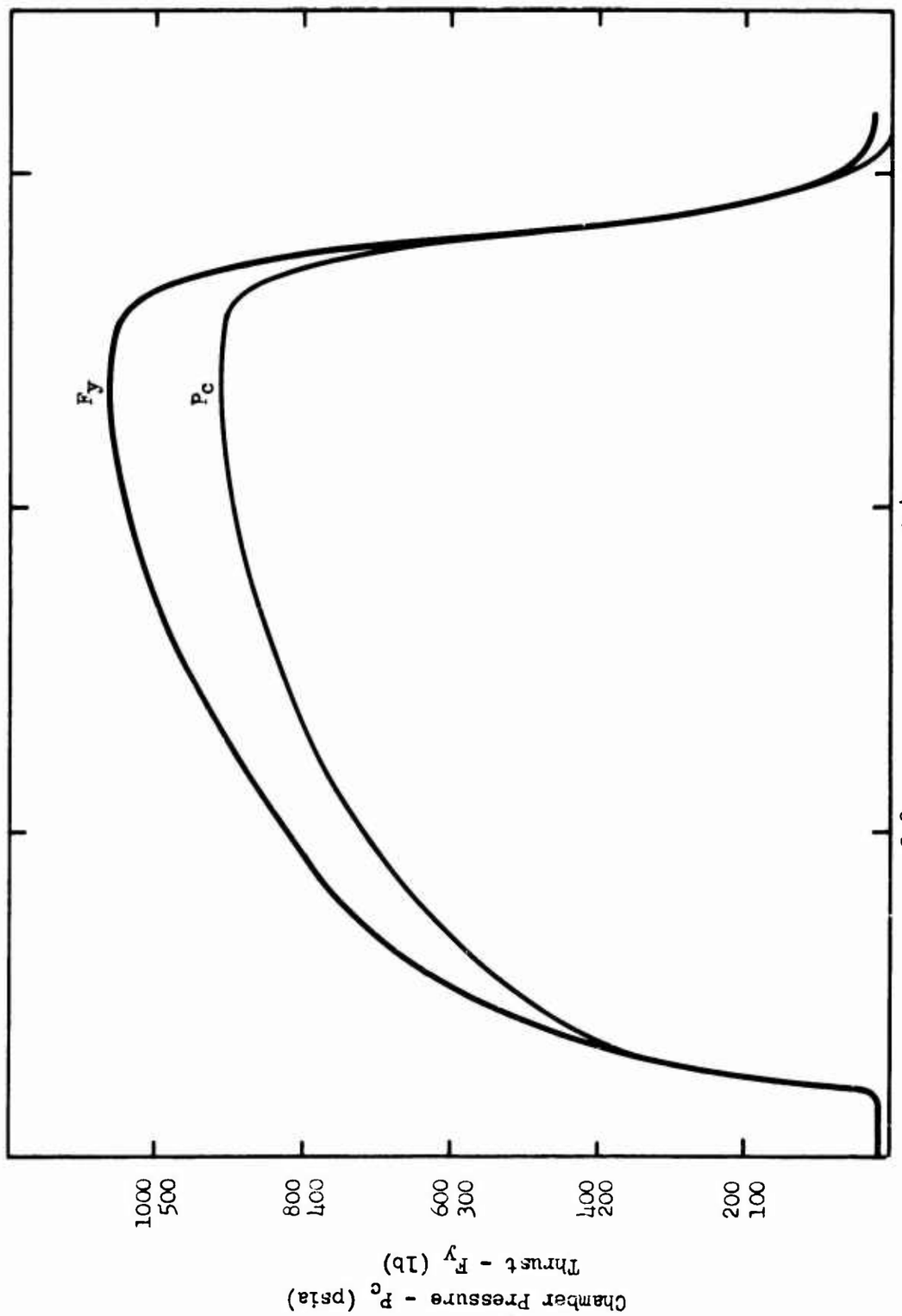

Motor Performance (Test Series FT-ZX-01S-BH-6)

Figure 14

TABLE 5

SUMMATION OF 1KS-250 MOTOR PERFORMANCE TEST RESULTS

TEST SERIES: FT-ZX-01S-BH-	1	2	3	4	5	6
PROPELLANT NO.	ANP 2969	ANP 2969	ANP 2969	ANP 2969	ANP 2969	ANP 3130
Test Date	12/7/65	12/10/65	1/7/66	1/25/66	1/25/66	2/18/66
Nozzle Flow Rate, lb/sec	0.775	0.733	0.723	Hang-fire	0.735	1.54
$\int Fd\theta$, lb-sec	258.8	239.5	259.2		258.0	228.8
I_s, sec^{-1}	221.4	221.2	221.3		221.3	253.9
I_s,(std), sec^{-1}	232.6	233.8	235.0		234.9	264.8
$\int p_c d\theta$,psia-sec	899	909	880		820	398.0
cw, sec	0.00657	0.00652	0.00656		0.0066	0.00589
θ, sec	1.509	1.600	1.620		1.584	0.585
$\overline{p_c}$ ave, psi	596	568	543		541	681
r_b, in./sec	0.283	0.268	0.271		0.264	0.963
C_f	1.46	1.44	1.45		1.46	1.50
Ae/At	7.290	7.290	7.076		6.952	7.111
At before/after $\sim$ $in.^2/in.^2$	0.196/0.200	0.196/0.201	0.201/0.205		0.205/0.207	0.407/0.362
C*	4900	4940	4920		4872	5470
C* efficiency	94.7	95.5	95.0		94.5	90.7
I_s theo (Shifting equil with solidif.)	262.2	262.2	262.6		262.6	314.1
I_s efficiency	88.8	89.1	89.6		89.5	84.3

The motor data reduction requires a calculation of the efficiency at motor conditions, i.e., Efficiency = $\frac{I_s \text{ measured at motor conditions}}{I_s \text{ theoretical at motor conditions}}$. This efficiency is then multiplied by the theoretical I_s computed at standard conditions to calculate an extrapolated I_s at standard conditions. In essence, the motor efficiency is assumed to remain constant over the range of conditions spanning actual motor conditions and standard conditions.

b. Temperature Measurements

A satisfactory measurement of particle temperature was accomplished in test firing No. 3 (Table 6). These measurements, however, were of low precision. No gas temperatures were measured because of a failure in the spectrometer scanning-power supply (apparently due to a microphonic output tube which failed as the motor fired).

TABLE 6

MEASURED TEMPERATURES ON 1KS-250 MOTOR NO. 3

Experiment No. 660107

Time, sec	Temperature, °K	Particle Cloud Emissivity	Particle Cloud Reflectivity
0.1	2804.0	0.2421	0.9907
0.2	2822.0	0.2575	0.9909
0.3	2845.0	0.2616	0.9925
0.4	2856.0	0.2679	0.9942
0.7	2899.0	0.2991	0.9975

The measurements, which indicate that the particles are still in the molten state, are an indication of conditions at the center of the plume. This is true because of the narrow "depth of field" of the receptor optical system, i.e., more light from the center of the plume strikes the detector than that from any other region.

The particle size distribution and number density used in the determination of emissivity were calculated from the light scattering and extinction measurements (described in the next section). Close agreement was achieved between the measured value of extinction coefficient at 0.588μ and that value calculated from the measured particle size (see Figures 15 and 16). As shown in Figure 15, the effective particle size changed during the firing, although the temperatures stated in Table 6 were calculated on the basis of the "time average" distribution of particle size shown by the dashed line in Figure 15, labeled "Firing No. 3."

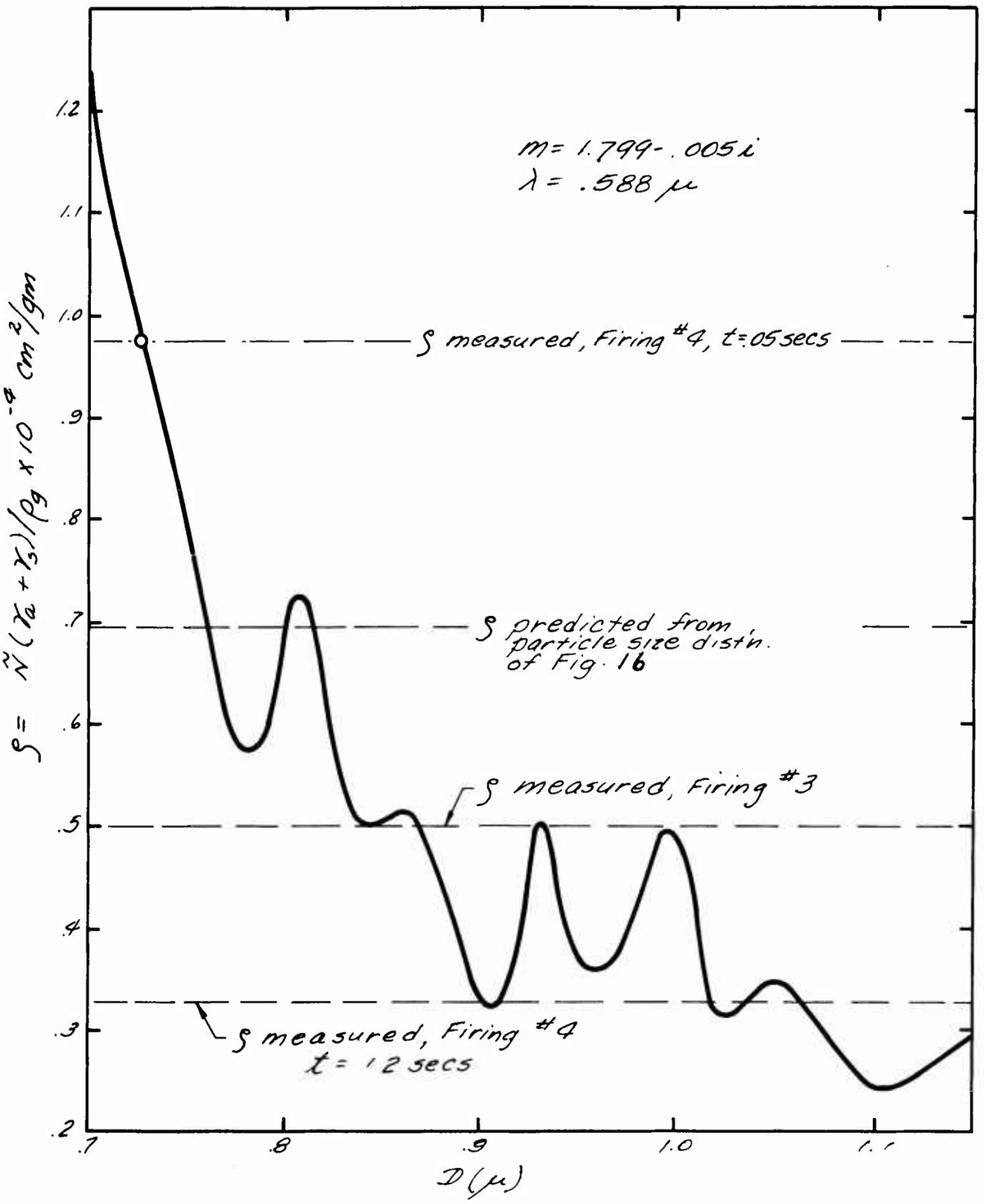

Specific Extinction Coefficient at $\lambda = 0.588\mu$

Figure 15

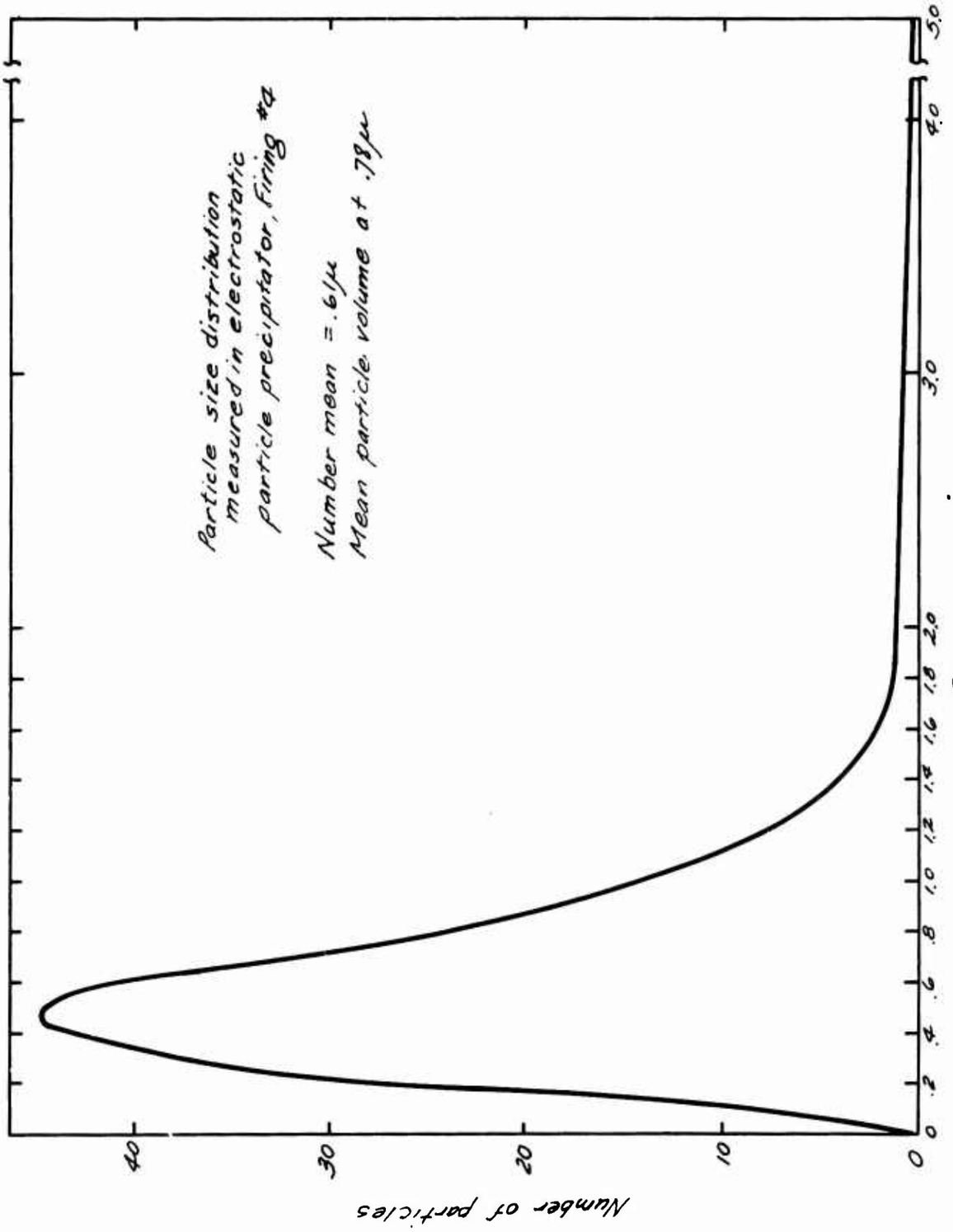

Particle Size Distribution from Particle Sampler,
Motor Firing No. 4

Figure 16

For the fourth motor firing, the apparatus was positioned again in the manner shown in Figure 7. In this test, successful measurements were made of both gas and particle temperature which are presented in Table 7. Theoretical temperatures for the one-dimensional and two-dimensional axisymmetric cases are shown in Table 8.

Although the scattering studies (discussed in the next section) could indicate only a time-averaged particle size distribution, the measured extinction coefficient at 0.588 to 0.589μ indicated that the effective particle size changed during the firing, as was the case in firing No. 3. This was accounted for in the calculations and the effective values of particle size are shown in Table 7.

The particle temperatures determined from measurements on firing No. 3 are higher than those for firing No. 4, a difference which cannot be due to random fluctuations. The measurements made on firing No. 3 were of much lower precision, as previously mentioned, because of an unknown plume emissivity. Data from test No. 3 were used to get sufficient gain on the recording channel to obtain a reasonable galvanometer deflection in firing No. 4.

It can be seen from Tables 7 and 8 that the measured gas temperature, although initially at a relatively low value (1958°K) rises during the firing to a level above that predicted for the shifting equilibrium case No. 6. The particle temperatures are also seen to rise, always remaining far above the melting temperature. Clearly, much thermal energy is being lost from the system in the form of sensible heat of the alumina, although the heat of fusion could not be expected to be recovered since the gas temperature is above the melting temperature.

More runs are necessary on similar motors to increase the statistical confidence in the measurements and eliminate the possibility of some heretofore unknown systemic bias which could cause erroneous measurements. However, there is no reason to doubt the validity of these measurements, and there are several possibilities which can account for the difference between the measured and theoretical temperatures. These are.

(1) Air is diffusing into and reacting with the gases in the exhaust plume. This phenomenon was observed to occur during radar attenuation studies (Reference 10) on exhaust plumes, where it accounted for appreciable increase in plume temperature. An analysis is presently under way to determine how extensive this effect could be for small motors. If assessed to be significant, the effect will be minimized through the use of a nitrogen "blanket" in subsequent exhaust plume studies.

(2) The departure from isentropic expansion will definitely be significant for a motor of the 1KS size. This effect will account for temperatures higher than theoretical, although the extent of irreversibility is difficult to assess by other than a knowledge of static temperature profiles.

TABLE 7

MEASURED TEMPERATURES ON 1KS-250 MOTOR NO. 4

Experiment No. 660125

Throat diameter: 0.512 in.

Aluminum loading: 0.738 moles Al/100 g

Measurement location: 12 mm downstream of exit plane

Expansion ratio at measurement location: 9.74

Plume thickness at measurement location: 4.43 cm

Time, sec	P_c, psia	T_p, °K	T_g, °K	Thermal Lag, °K	D*, Micron
0.05	415	2387	1958	429	0.731
0.10	420	2408	2119	289	0.752
0.15	455	2411	2181	230	0.765
0.20	460	2383	2221	162	0.821
0.25	465	2415	2273	142	0.823
0.30	475	2438	2307	131	0.825
0.40	500	2481	2359	122	0.830
0.50	520	2517	2371	146	0.840
0.60	550	2535	2373	162	0.872
0.70	570	2538	2355	183	0.880
0.80	590	2557	2334	223	0.885
0.90	610	2570	2273	297	0.895
1.00	640	2593	2253	340	0.895
1.20	690	2643	2283	360	0.895

TABLE 8

THEORETICAL TEMPERATURES FOR 1KS-250 MOTORS AT MEASUREMENT STATION

One-dimensional case, P_c = 400-1000 psia

Expansion ratio - 9.74

Condition[1]	Temperature, °K (Assuming no thermal lag)
1	1810
2	1880
3	2020
4	2100
5	2160
6	2277

Axisymmetric case[2], determination of radial temperature profile at ε_y = 9.74:

	Temperature, °K		
P_c	Center	Minimum Temp.	Edge
700	2000	1970	2319
400	2130	2090	2460

1 Conditions in one-dimensional computation:

1 - Frozen equilibrium at chamber with supercooling of particles

2 - Frozen equilibrium at throat with supercooling of particles

3 - Frozen equilibrium at chamber with solidification of particles

4 - Frozen equilibrium at throat with solidification of particles

5 - Shifting equilibrium with supercooling of particles

6 - Shifting equilibrium with solidification of particles

2 Estimate for shifting equilibrium with supercooling. These numbers serve only to indicate the radial temperature profile across the plume.

(3) The unexpected rise in temperature during the firing may have been caused by a partial plugging of the nozzle during ignition. Such an effect has been observed in other motors, particularly where a fast ignition transient occurs as was the case here.

(4) Disequilibrium between the sodium and the surrounding gas could account for a higher observed temperature; however, a conservative estimate of the extent of this effect would account for an increase of less than 10°K, thus eliminating this as a primary cause.

(5) The uncertainty in the thermodynamic data, which must be used to establish the composition of the gas and the relationship between the internal energy of the gas and its temperature, could account for approximately one-half of the observed difference between the theoretical and measured temperatures (Reference 11).

c. Scattering Measurements

Figure 17 presents the measurements made on light scattering on the motor in firings No. 3 and No. 4, together with the curve calculated from Mie scattering theory for the particle size distribution shown in Figure 16. The distribution shown in Figure 16 was the result of micrographic examination of a sample of particles taken in the plume during firing No. 4.

The light source used for the light scattering measurements is a high-intensity, water-cooled BH-6 mercury arc lamp, the beam from which is focused at the center of the exhaust plume at a position 1.25 in. downstream from the exit plane. The detectors are positioned to intercept light in the plane of polarization which lies perpendicular to the plume centerline (i_2, Reference 2). These detectors are placed approximately 7-in. from the plume centerline at angles of 0°, 57.5°, and 120.5° to the incident beam.

Light striking the phototube detectors was filtered by means of a narrow-band interference filter centered at 0.436μ (Reference 2). The emf recorded from the detectors was coupled through an RC network to an amplifier and galvanometer. Because the reflected light from the mercury arc was of lower intensity than emission fluctuations from the flame, the recorded emf was basically of an erratic, random character and had superimposed on it a 120-cps wave representing the light reflected from the mercury arc lamp. Only averaged values of reflected light for the entire run could be obtained, because of the number of data required to discriminate the reflected emf through a regression analysis. The particle size distribution of Figure 16, obtained from the particle sampler, would also represent a time-averaged value.

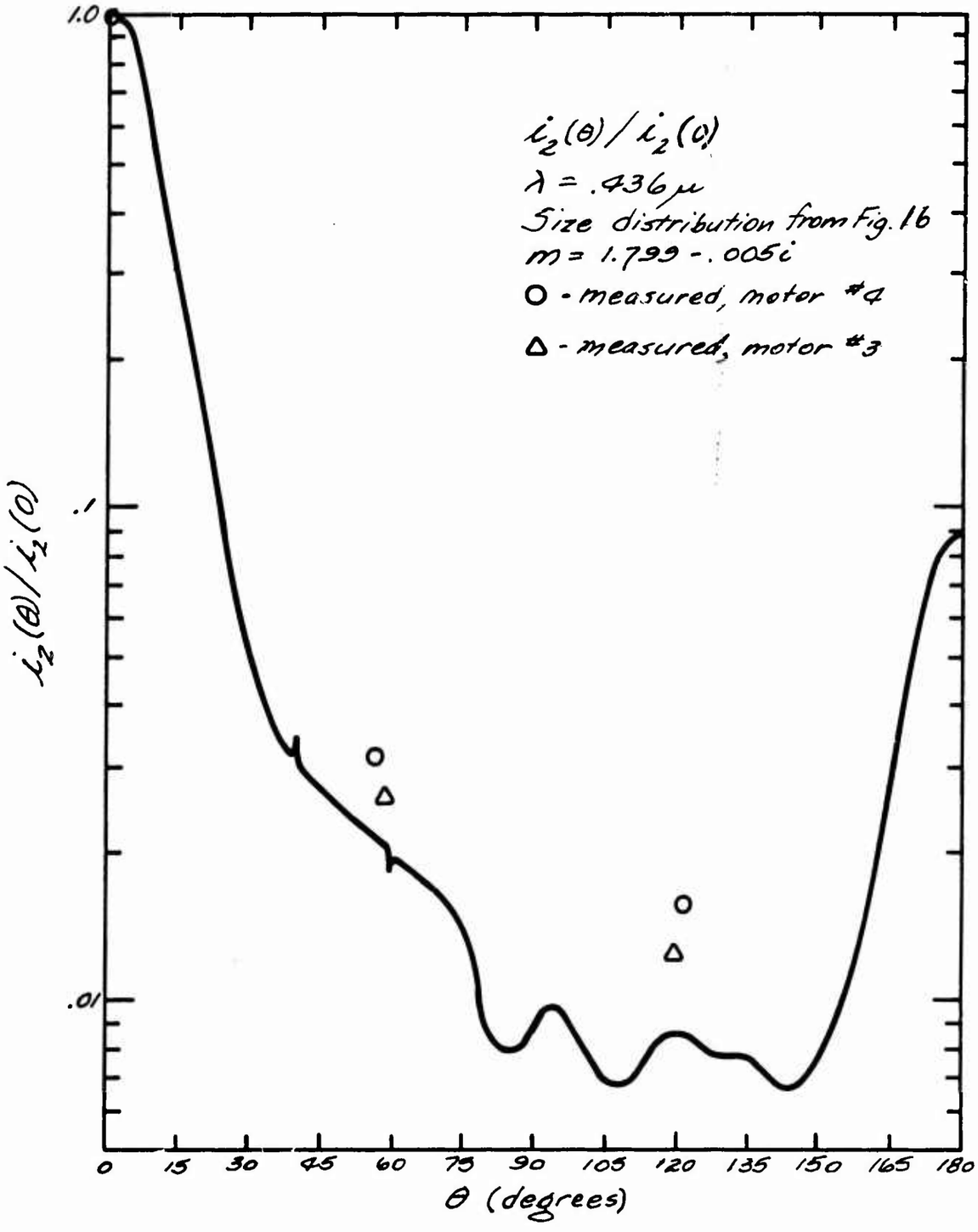

Light Scattering Diagram, $i_2(\Theta)/i_2(0)$, $\lambda = 0.436\mu$

Figure 17

The four data points presented in Figure 17 for the angles 57.5° and 120.5° are of very low precision because of the relatively low intensity of the scattered light at these angles. In fact, from the regression analysis, there is less than 5% confidence that the 120-cps signal actually accounts for the reported data points. That is, the measured signal could be stated as being completely random with greater than 95% confidence.

This is not the case with the measurement at 0° however; there, the difference between a completely random signal and the observed signal is due to the superimposed 120 cps with a confidence level greater than 99% for both firings. For this reason, the extinction coefficient was determined from the measurement at 0° and is presented in Figure 18, together with values calculated for a monodispersed distribution.

It is concluded from the scattering measurements that a light source is needed with a spectral radiance 10 to 15 times greater than the mercury arc lamp, in order to obtain even minimal precision on the scattering measurements on optically thick plumes. An optical maser would be an ideal tool for this application.

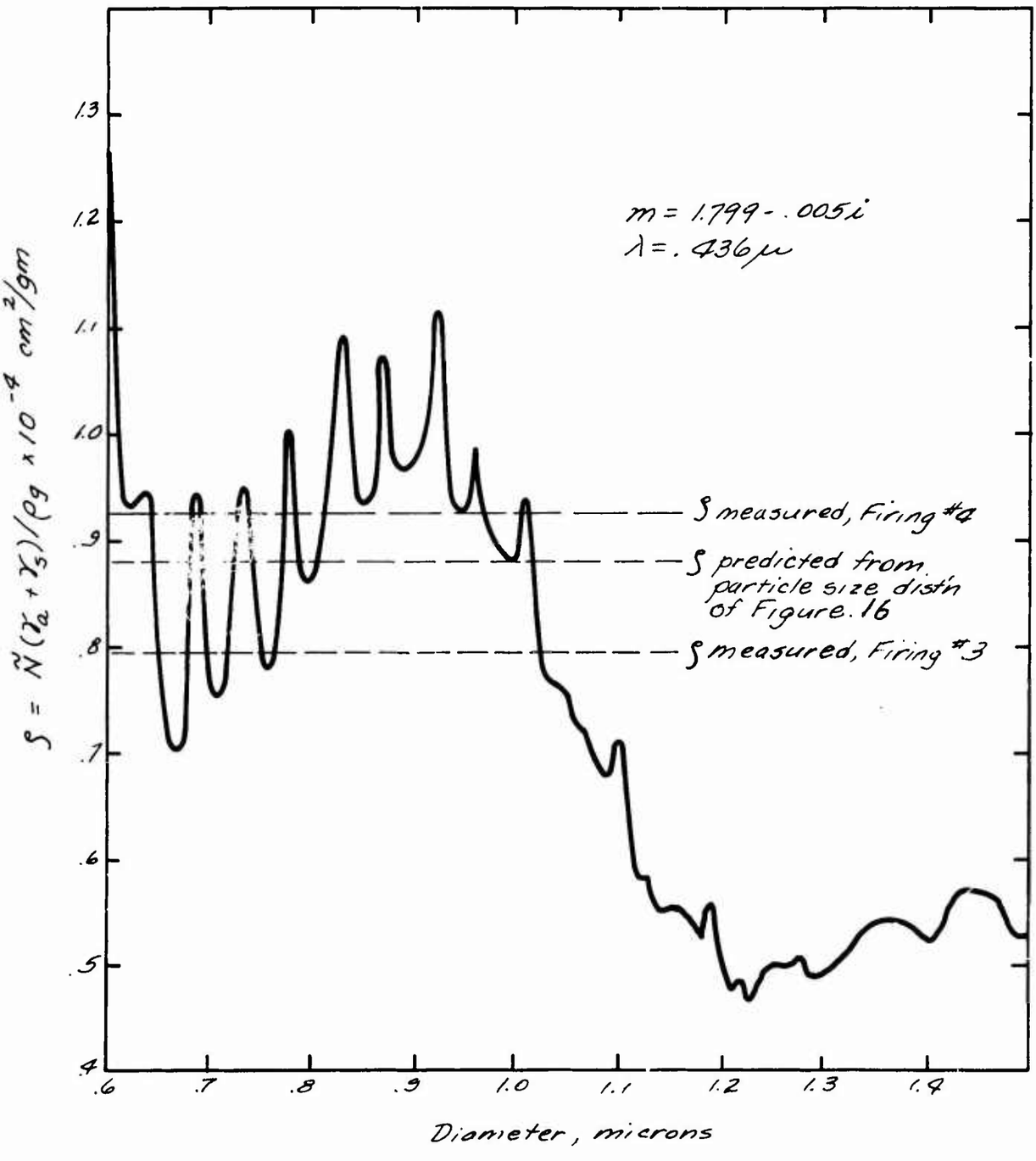

Specific Extinction Coefficient at $\lambda = 0.436\mu$

Figure 18

III.

SUMMARY OF PRESENT STATUS

To date a total of five motors have been tested. The first group of three motors, which contained the aluminized propellant ANP 2969, was tested in December and early January.

The temperature data obtained from the first two motor tests indicated a loss in precision which results from insufficient intensity of the reference light source. Since the source intensity is reduced approximately 80% by the rotating mirror--penta prism--fiber bundle path, prior to entering the motor exhaust plume, the carbon arc light source was moved directly to the exhaust plume for the third test, bypassing the optical switching equipment and hence precluding simultaneous chamber and exhaust temperature measurements. The third test was then conducted with exhaust temperature measurements only, together with exhaust scattering measurements using a mercury arc light source. Following these, a substitute test was conducted, with RPL concurrence, which permitted a fourth motor with aluminized propellant to be tested in place of the first toxic test motor containing the LM-2 propellant ANP 2991 HG Mod IA.

At the completion of the fourth test, a meeting was held at Edwards AFB with RPL program personnel on 3 February 1966, to determine the best direction for the remaining 1KS-250 motor tests. The following direction was mutually agreed upon:

1. To conduct scattering and temperature measurements with the carbon arc light source in the chamber using the four port aft closures. Fire one motor with LMH-2 propellant and then two motors in immediate succession, one each with LM-2 and LMH-2 propellants. Exhaust plume scattering studies will also be conducted using an alternate light source (e.g., mercury arc, Xenon discharge tube, or Ruby laser).

2. If above chamber scattering measurements using the carbon arc light source are successful, test two motors in immediate succession, one motor each of LM-2 and LMH-2 propellants, taking temperature and scattering measurements in the exhaust plume only. If tests in 1 above are not successful, test one each LM-2 and LMH-2 motors with chamber scattering and exhaust temperature measurements, using an alternate light source in the chamber and the carbon arc light source in the exhaust.

The fifth motor test was conducted on 18 February 1966 with the LMH-2 propellant, ANP 3130.

On 21 February 1966, the remaining tests were temporarily stopped by RPL until optical maser equipment is shipped from the Rocket Propulsion Laboratory and checked out at Aerojet to determine whether it can be developed into a reference light source for chamber temperature measurements in this program. The majority of the required components for this light source are part of the optical maser assembly.

The nozzle and test motor fabrication together with the optical viewports have been completed for all of the remaining 1KS-250 size motors to be tested during the program. Fabrication of all component parts was completed. Three grains of the LMH-2 propellant (ANP 3130) were prepared from 1 -lb batches for the third group of motor tests. LM-2 propellant processing for the second group of motor firings using ANB 3084 was terminated. The LM-2 propellant was changed back to the originally proposed propellant, ANP 2991 HG, and no processing difficulties were experienced. Five grains have been cast, cured, and await testing.

IV.

PLANNED FUTURE WORK

1. The remaining tests have been temporarily postponed until the components for the pulsed Xenon light source are developed. Components for this light source will be obtained early in March, and checked out to determine what modifications, if any, will be necessary to allow chamber temperature to be measured. In the event these modifications are very costly, in both time and money, the testing program may be resumed using the pulsed Xenon light source for exhaust plume scattering studies only.

2. Redesign and incorporate modifications to the auxiliary equipment data ranging system to accommodate extreme differences in signal strength between the pulsed Xenon light source and plume radiancy.

3. Complete the data reduction and analysis of the tests conducted thus far.

4. Conduct the remaining toxic motor tests with both the LM-2 and LMH-2 propellants.

5. Prepare draft of final report and submit to RPL for approval.

V.

NOMENCLATURE

c^* - Characteristic exhaust velocity, ft/sec

C_2 - Constant, Plancks law = 14388 $\mu\ ^\circ K$

E_{c^*} - Characteristic exhaust velocity efficiency

$E_{I_{sp}}$ - Impulse efficiency--measured/theoretical

E_{i_j} - Galvanometer deflection at the i^{th} wavelength

E_T - Thermal efficiency

j = 1 refers to condition with reference source on

j = 2 refers to condition with reference source off

j = 0 refers to condition with only reference source

F_y - Measured motor thrust, lb force

K_{i_j} - Phototube-system constant

m - Refractive index

n - Real part, refractive index

n' - Imaginary part, refractive index

$\tilde{N}$ - No. density of particles, cm^{-3}

P_c - Chamber pressure, psia

r - Radius of particle, cm

T - Temperature, $^\circ K$

t - Cloud thickness, optical pathlength, cm

V - Mean particle volume

GREEK

γ - Cross section, cm^2

ε - Emittance, expansion ratio

$\bar{\varepsilon}$ - Average emittance

λ - Wavelength,

ρ - Density, gm/cm^3

χ - Mass fraction of particles

ϕ - Frequency function

σ - Time, sec

SUBSCRIPTS

al - Absorption, at λ_1

b - Brightness

g - Gas

l - Liquid

sl - Scattering, at λ_1

VI.

REFERENCE

1. Colucci, S. E. and Adams, J. M. "Flame Temperature Measurements in Metallized Propellant," Aerojet General Corporation, Aug. 1965.

2. Colucci, S. E. and Adams, J. M. "Flame Temperature Measurements in Metallized Propellant," Aerojet General Corp., Report SRO 20, Nov. 1965.

3. Erickson, W. D., "Light Scattering: A Technique for Studying Soot in Flames," Ph.D. Thesis in Chemical Engineering, MIT, Dec. 1961.

4. Malitson, I. H. et al. "Refractive Index of Synthetic Sapphire," J. Opt. Soc. Am. 48, No. 1, Jan. 1958.

5. Gryvnak, D. A. and Burch, D. E. "Optical and Infrared Properties of Al_2O_3 at Elevated Temperatures," Philco Pub. No. U-2623, May 1964.

6. Carlson, D. J. and R. A. Dupuis, "Alumina Absorption and Emittance," Philco Pub. No. 2627, May 1964.

7. Coughlin, J. P. and Smith, R. M., "A Description of the Aerojet-General Corporation Computer Program for Calculation of Specific Impulse and Related Variables," AGC Technical Publication, Feb. 1963.

8. Kirshenbaum, A. D. and Cahill, J. A. "The Density of Liquid Aluminum Oxide," J. Inorg. Nucl. Chem. 14, (1960), 283-287.

9. Kuby, W., et al., "An Investigation of Recombination and Particle Lags Effects in Rocket Nozzle," (U) Aeronutronic Report C-1938, Confidential, December 1962.

10. Coughlin, J. P. and Hollingsworth, S. W. "A correlation between Measured and Computed Values of Microwave Attenuation for Solid Propellant Exhausts Part II: Theoretical Calculations and Correlations," Special Session, 20th Interagency Solid Propellant Meeting, Philadelphia, Penn., July 1964 (Volume IV, Bulletin).

11. Coughlin, J. P., Personal Communication with J. M. Adams, March 1966.

12. JANAF Thermochemical Data, The DOW Company Thermal Laboratory, Midland, Michigan, 31 December 1960, and subsequent revisions.

APPENDIX

DETERMINATION OF n' FROM MEASUREMENTS OF PARTICLE CLOUD EMISSION

It has been shown in the body of this report that n', the imaginary part of the refractive index, has a strong effect on the calculated value of particle cloud emissivity. For this reason, studies have been devoted to the determination of n' for molten alumina. These studies have included laboratory measurements on emission of optically thin flames containing molten alumina, and reduction of data previously reported in the literature.[1]

The absorption cross section is related to the emissivity and hence the radiancy of a particle cloud by (Equation 4 of the main text):

$$E_{12}K_{12} = \frac{1 - \exp(\tilde{N}\gamma_{a_1} t)}{\lambda_1^5\left[\exp\left(\frac{C_2}{\lambda_1 T_p}\right) - 1\right]} \qquad \text{(Eq 1)}$$

or, for the optically thin case ($\tilde{N}\gamma_a t \ll 1$)

$$E_{12}K_{12} = \frac{\tilde{N}\gamma_{a_1} t}{\lambda_1^5\left[\exp\left(\frac{C_2}{\lambda_1 T_p}\right) - 1\right]} \qquad \text{(Eq 2)}$$

If the solid angle which the spectrometer-detector subtends of the particle cloud is the same as that which it subtends of a reference light source image, we have:

$$E_{10}K_{10} = \frac{1}{\lambda_1^5\left[\exp\left(\frac{C_2}{\lambda_1 T_b}\right) - 1\right]} \qquad \text{(Eq 3)}$$

where T_b is the brightness temperature of the reference light source image in the flame. The phototube-system constant, K_{ij}, which may be a function of both wavelength and E_{ij}, can be determined by using various brightness temperatures in Equation 3. From Equation 2, the relation for γ_{a1} becomes:

---

1. Carlson, D. J. and R. A. Dupuis, "Alumina Absorption and Emittance," Philco Publication No. 2627, May 1964

$$\gamma_{al} = \frac{E_{12}K_{12}}{\tilde{N}\,t}\,\frac{\lambda_1^5}{\left[\exp\left(\frac{C_2}{\lambda_1 T_p}\right) - 1\right]} \qquad \text{(Eq 4)}$$

The number density of particles is determined from a knowledge of particle size distribution, the mass fraction of particles in the two phase flow field and the particle and gas densities, i.e.,

$$\tilde{N} = \frac{\chi\bar{\rho}}{\rho_L\ \bar{V}}$$

$$= \frac{\rho_g\ \chi}{\left[\rho_g \chi + \rho_L (1 - \chi)\right]\ \bar{V}} \qquad \text{(Eq 5)}$$

The mass fraction of particles for the above was determined from data obtained during the experiments on mass flow rates of particles into the flame and gas flow rates (v. Reference 2).

Another relation of use to the calculation is that which describes the transmission of radiation through the plume from the reference light source (Equation 5).

$$E_{11}K_{11} - E_{12}K_{12} = \frac{\exp\left(\tilde{N}(\gamma_{al} + \gamma_{sl})t\right)}{\lambda_1^5\left[\exp\left(\frac{C_2}{\lambda_1 T_b}\right) - 1\right]} \qquad \text{(Eq 6)}$$

which together with Equation 3, gives:

$$\tilde{N}(\gamma_{al} + \gamma_{sl})t = \ln\left[\frac{E_{11}K_{11} - E_{12}K_{12}}{E_{10}K_{10}}\right] \qquad \text{(Eq 7)}$$

Using Equation 4, then, γ_{al} was calculated for the particular set of conditions which existed during the measurement. γ_{sl} was determined for the given particle size distribution at various n and n'. Equation 7 was then used as a check on the values of $\tilde{N}$, γ_{al}, and γ_{sl}.

The particle temperature was assumed to be equal to the measured gas temperature for these results. A difference of 50°K between the two temperatures would still result in a change in γ_a less than the cumulative uncertainties in the experiment.

To obtain the results of Table 4 of the main text, the values of $\bar{\varepsilon}$ presented in Reference 6 were used. $\bar{\varepsilon}$ is related to the absorption cross section through the following (Reference 6).

$$\bar{\varepsilon} = \frac{\int_0^\infty \varepsilon(r)\, \phi(r)\, \pi r^2 dr}{\int_0^\infty \phi(r)\, \pi r^2 dr}, \qquad \text{(Eq 8)}$$

where $$\varepsilon(r) = Q^a(r) = \frac{\gamma_a(r)}{\pi r^2}. \qquad \text{(Eq 9)}$$

Therefore

$$\bar{\varepsilon} = \frac{\int_0^\infty \gamma_a(r)\, \phi(r)\, dr}{\int_0^\infty \phi(r)\, \pi r^2 dr}, \qquad \text{(Eq 10)}$$

where $\phi(r)$ is the frequency factor, normalized such that

$$\int_0^\infty \phi(r) dr = 1. \qquad \text{(Eq 11)}$$

The values of $\phi(r)$, obtained from Figure 3 of Reference 6, are given in Table 1.

TABLE 1

PARTICLE SIZE DISTRIBUTION FROM REFERENCE 6

r, microns	ϕ (r), micron -1
0.278	0.724
0.556	1.110
0.834	0.766
1.112	0.366
1.390	0.226
1.668	0.158
1.946	0.094
2.224	0.059
2.502	0.034

The calculated value of

$$\bar{\pi r^2} = \int_0^{\infty} \phi\ (r)\, \pi\ r^2\ dr\ =\ 2.74 \times 10^{-8}\ cm^2$$

This value differs from that calculated in Reference 6 (which gave a value of 6.5×10^{-8} cm^2), but was consistent with the means of calculating γ_a (r) using Simpson's rule on the nine points of the distribution.

$\bar{\gamma}_a$, the average absorption cross section for the particle size distribution is given by

$$\bar{\gamma}_a = \int_0^{\infty} \gamma_a(r) \phi\ (r)\ dr \qquad \text{(Eq 12)}$$

and is related to the $\bar{\varepsilon}$ of Reference 6 by

$$\bar{\gamma}_a = \bar{\varepsilon} \int_0^{\infty} \phi\ (r)\ \pi\ r^2\ dr \qquad \text{(Eq 13)}$$

$$= 2.74 \times 10^{-8}\ \bar{\varepsilon} \qquad \text{(Eq 14)}$$

Values of $\bar{\varepsilon}$ were obtained by constructing a straight line through the data of Figure 12 of Reference 6 above 2320°K. The $\bar{\gamma}_a$ were then calculated at various temperatures from Equation 14.

To determine the proper values of n', the equation

$$\bar{\gamma}_a = \int_0^\infty \gamma_a (r, n') \phi (r) \, dr$$

was used at λ = 1.3 and 1.7 μ . This resulted in the values given in Table 4 of the main text.

NOMENCLATURE

C_2 - Constant, Plancks law = 14388 μ °K

E_{ij} - Galvanometer deflection at the i^{th} wavelength

j = 1 refers to condition with reference source on

j = 2 refers to condition with reference source off

j = 0 refers to condition with only reference source

K_{ij} - Phototube-system constant

m - Refractive index

n - Real part, refractive index

n' - Imaginary part, refractive index

$\tilde{N}$ - No. density of particles, cm^{-3}

r - Radius of particle, cm

T - Temperature, °K

t - Cloud thickness, optical pathlength, cm

$\bar{V}$ - Mean particle volume = $\int_0^\infty V(r)\,\phi\,(r)dr$

GREEK

γ - Cross section, cm^2

ϵ - Emittance

$\bar{\epsilon}$ - Average emittance

λ - Wavelength, micron

ρ - Density, gm/cm^3

χ - Mass fraction of particles

ϕ - Frequency function

SUBSCRIPTS

al - Absorption, at λ_1

b - Brightness

g - Gas

l - Liquid

sl - Scattering, at λ_1

Report AFRPL-TR-66956

AFSCR 80-20

Unclassified

Security Classification

DOCUMENT CONTROL DATA - R&D

(Security classification of title, body of abstract and indexing annotation must be entered when the overall report is classified)

1 ORIGINATING ACTIVITY (Corporate author) Aerojet-General Corporation Sacramento, California 95809	2a REPORT SECURITY CLASSIFICATION Unclassified 2b GROUP N/A

3 REPORT TITLE

Flame Temperature Measurement of Metallized Propellant

4 DESCRIPTIVE NOTES (Type of report and inclusive dates)

3rd Quarterly Progress Report, 19 Nov. 1965 - 18 Feb 1966

5 AUTHOR(S) (Last name, first name, initial)

Colucci, Steve E.
Adams, Jim M.

6 REPORT DATE	7a TOTAL NO OF PAGES	7b NO OF REFS
March 1966	51	12

8a CONTRACT OR GRANT NO.	9a ORIGINATOR'S REPORT NUMBER(S)
AF 04(611)10545 b PROJECT NO 3148 PRSN 314803 c Program Structure No. 750G d	AFRPL-TR-66956
	9b OTHER REPORT NO(S) (Any other numbers that may be assigned this report) None

10 AVAILABILITY/LIMITATION NOTICES

Foreign announcement and dissemination of this report by DDC is not authorized.

11 SUPPLEMENTARY NOTES	12 SPONSORING MILITARY ACTIVITY
None	Air Force Rocket Propulsion Lab (RPCL) Edwards AFB, Calif. 93523

13 ABSTRACT

This third quarterly technical report under Contract AF 04(611)10545 presents a discussion of the Flame Temperature Measurement program progress, since the previous quarterly report. The objective of this program is to develop the techniques for flame temperature measurement of metallized propellants. The program includes laboratory development of the temperature measurement technique, test motor development, and results of 1KS-250 motor tests.

Results of laboratory measurements of spectral absorption cross sections are presented and are used to calculate values of the imaginery part of the refractive index for molten alumina. Other results, obtained from the literature are also used as a comparison.

A discussion of the experimental program using small solid rocket motors is presented. The experimental effort includes results of light scattering studies, and gas and particle temperature measurements on the exhaust plume of these small motors.

DD FORM 1 JAN 64 1473

UNCLASSIFIED

Security Classification

AFSCR 80-20
Unclassified

Security Classification

14 KEY WORDS	LINK A		LINK B		LINK C	
	ROLE	WT	ROLE	WT	ROLE	WT
1. Spectral Comparison Pyrometer						
2. Refractive index for Alumina						
3. Flame Temperature Measurement						
4. Light Scattering Studies						
5. Condensed Specie (particle) Temperature						
6. Spectroscopic Measurements						
7. Mie Scattering Theory						
8. Particle Cloud Emission						

INSTRUCTIONS

1. ORIGINATING ACTIVITY: Enter the name and address of the contractor, subcontractor, grantee, Department of Defense activity or other organization *(corporate author)* issuing the report.

2a. REPORT SECURITY CLASSIFICATION: Enter the overall security classification of the report. Indicate whether "Restricted Data" is included. Marking is to be in accordance with appropriate security regulations.

2b. GROUP: Automatic downgrading is specified in DoD Directive 5200.10 and Armed Forces Industrial Manual. Enter the group number. Also, when applicable, show that optional markings have been used for Group 3 and Group 4 as authorized.

3. REPORT TITLE: Enter the complete report title in all capital letters. Titles in all cases should be unclassified. If a meaningful title cannot be selected without classification, show title classification in all capitals in parenthesis immediately following the title.

4. DESCRIPTIVE NOTES: If appropriate, enter the type of report, e.g., interim, progress, summary, annual, or final. Give the inclusive dates when a specific reporting period is covered.

5. AUTHOR(S): Enter the name(s) of author(s) as shown on or in the report. Enter last name, first name, middle initial. If military, show rank and branch of service. The name of the principal author is an absolute minimum requirement.

6. REPORT DATE: Enter the date of the report as day, month, year; or month, year. If more than one date appears on the report, use date of publication.

7a. TOTAL NUMBER OF PAGES: The total page count should follow normal pagination procedures, i.e., enter the number of pages containing information.

7b. NUMBER OF REFERENCES: Enter the total number of references cited in the report.

8a. CONTRACT OR GRANT NUMBER: If appropriate, enter the applicable number of the contract or grant under which the report was written.

8b, 8c, & 8d. PROJECT NUMBER: Enter the appropriate military department identification, such as project number, subproject number, system numbers, task number, etc.

9a. ORIGINATOR'S REPORT NUMBER(S): Enter the official report number by which the document will be identified and controlled by the originating activity. This number must be unique to this report.

9b. OTHER REPORT NUMBER(S): If the report has been assigned any other report numbers *(either by the originator or by the sponsor)*, also enter this number(s).

10. AVAILABILITY/LIMITATION NOTICES: Enter any limitations on further dissemination of the report, other than those imposed by security classification, using standard statements such as:

(1) "Qualified requesters may obtain copies of this report from DDC."

(2) "Foreign announcement and dissemination of this report by DDC is not authorized."

(3) "U. S. Government agencies may obtain copies of this report directly from DDC. Other qualified DDC users shall request through

_____."

(4) "U. S. military agencies may obtain copies of this report directly from DDC. Other qualified users shall request through

_____."

(5) "All distribution of this report is controlled. Qualified DDC users shall request through

_____."

If the report has been furnished to the Office of Technical Services, Department of Commerce, for sale to the public, indicate this fact and enter the price, if known.

11. SUPPLEMENTARY NOTES: Use for additional explanatory notes.

12. SPONSORING MILITARY ACTIVITY: Enter the name of the departmental project office or laboratory sponsoring *(paying for)* the research and development. Include address.

13. ABSTRACT: Enter an abstract giving a brief and factual summary of the document indicative of the report, even though it may also appear elsewhere in the body of the technical report. If additional space is required, a continuation sheet shall be attached.

It is highly desirable that the abstract of classified reports be unclassified. Each paragraph of the abstract shall end with an indication of the military security classification of the information in the paragraph, represented as *(TS)*. *(S)*. *(C)*. *or (U)*

There is no limitation on the length of the abstract. However, the suggested length is from 150 to 225 words.

14. KEY WORDS: Key words are technically meaningful terms or short phrases that characterize a report and may be used as index entries for cataloging the report. Key words must be selected so that no security classification is required. Identifiers, such as equipment model designation, trade name, military project code name, geographic location, may be used as key words but will be followed by an indication of technical context. The assignment of links, rules, and weights is optional.

Unclassified

Security Classification